Simulation method for assessing hourly energy flows in district heating system with seasonal thermal energy storage

Narula, Kapil; de Oliveira Filho, Fleury; Villasmil, Willy; Patel, Martin

How to cite

NARULA, Kapil et al. Simulation method for assessing hourly energy flows in district heating system with seasonal thermal energy storage. In: Renewable Energy, 2019, p. 1–19. doi: 10.1016/j.renene.2019.11.121

This publication URL: https://archive-ouverte.unige.ch/unige:129062
Publication DOI: 10.1016/j.renene.2019.11.121

Renewable Energy xxx (xxxx) xxx

Contents lists available at ScienceDirect

Renewable Energy

journal homepage: www.elsevier.com/locate/renene

Simulation method for assessing hourly energy flows in district heating system with seasonal thermal energy storage

Kapil Narula [a, *], Fleury de Oliveira Filho [b], Willy Villasmil [c], Martin K. Patel [a]

[a] Chair for Energy Efficiency, Department F.-A. Forel for Environmental and Aquatic Sciences (DEFSE), Institute for Environmental Sciences (ISE), Faculty of Science, University of Geneva, Switzerland
[b] Energy Systems Group, Department F.-A. Forel for Environmental and Aquatic Sciences (DEFSE), Institute for Environmental Sciences (ISE), University of Geneva, Switzerland
[c] School of Engineering and Architecture, Lucerne University of Applied Sciences and Arts, 6048, Horw, Switzerland

ARTICLE INFO

Article history:
Received 17 July 2019
Received in revised form
12 November 2019
Accepted 23 November 2019
Available online xxx

Keywords:
Seasonal thermal energy storage (STES)
Sensible heat
Solar thermal
District heating (DH)
Modelling
Simulation

ABSTRACT

Domestic hot water and space heating demand in buildings contribute a high share of final energy demand. This demand is often met by fossil fuels, leading to large greenhouse gas emissions. Although renewable energy can be used for heating, there is time discordance between heat supply and heat demand. Seasonal thermal energy storage is a viable solution to overcome this mismatch. This paper presents a simulation method and a simple tool to assess the feasibility of integrating a seasonal thermal energy storage equipped with heat exchangers and/or heat pumps in a district heating system. The developed method and tool are generic and allow the simulation of hourly energy flows using energy balances and predefined conditions. In order to validate the proposed method, the result of the simulated energy flows from two selected systems, Friedrichshafen and Marstal, are compared with monitored values reported in literature. The comparison shows that while simulation of monthly energy flows depends on the accuracy of inputs to the tool, annual energy flows can be closely replicated. Hence, the method can be considered as validated. This simulation tool and method can be used to assess energy flows in a district heating system in future.

1. Introduction

Space heating (SH) and domestic hot water (DHW) production in buildings contributed to about 60% (36 EJ) of final energy demand in countries[1] with cold climate and about 43% (24 EJ) in countries in moderate and warm climate in 2010 [1]. In Europe the situation was similar and heating contributed to 80% (SH-65% and DHW-15%) of the final energy demand in the residential sector in 2016 in EU-28 countries [2]. On the supply side, 54% of heat in buildings was provided by fossil fuel boilers and 24% was supplied by electric heaters in 2017 [3]. The remaining heat was supplied by district heating (DH) (12%), renewable energy (RE) (8%) and heat pumps (HPs) (2%) [3]. Thus, on one hand heating contributes to a large share of energy demand and on the other, it is dependent on fossil fuels thereby leading to large greenhouse gas (GHG) emissions. In order to lower emissions, countries agreed on global peaking of GHG emissions, 'as soon as possible', and attaining GHG emissions neutrality in the second half of the century as a part of the Paris climate agreement in 2015 [4]. Hence, it is important to decarbonise the heating sector.

Heat demand in buildings is seasonal in nature with peaks in winter months, while RE is intermittent and excess solar energy is often available in summer months. This leads to a time discordance between heat supply and demand. In periods of low heat demand, excess heat may also be available from waste incinerators, industrial heat rejects, low temperature heat from waste water treatment plants and data centres. Thermal energy storage (TES) is a viable solution to overcome the mismatch between heat supply and demand as it can store heat on an hourly, daily, weekly and seasonal basis thus contributing to a global energy transition [5]. Seasonal thermal energy storage (STES) is being increasingly used to facilitate fluctuating RE production and it is estimated that more than 90% of the globally installed thermal storage capacity was used for capacity firming and time shifting of energy generated from RE in

* Corresponding author.
E-mail address: Kapil.Narula@unige.ch (K. Narula).

[1] OECD countries excluding Australia, Mexico, New Zealand and Israel, and non-OECD countries in Europe and Eurasia.

https://doi.org/10.1016/j.renene.2019.11.121
0960-1481/

Abbreviations

ATES	Aquifer thermal energy storage
BTES	Borehole thermal energy storage
COP	Coefficient of Performance
CSHPSS	Central solar heating plants with seasonal storage
DH	District heating
DHW	Domestic hot water
EINSTEIN	Effective integration of seasonal thermal energy storage systems in existing buildings
GHG	Greenhouse gas
HE	Heat exchanger
HP	Heat pump
ORC	Organic Rankine cycle
PES	Primary energy supply
PTES	Pit thermal energy storage
RE	Renewable energy
SH	Space heating
STES	Seasonal thermal energy storage
TES	Thermal energy storage
TRNSYS	Transient system simulation tool
TTES	Tank thermal energy storage
WGTES	Water gravel thermal energy storage

Nomenclature

B	Width of the PTES at base [m]
COP_{Carnot}	Carnot efficiency [%]
COP_{max}	Maximum COP of HP [−]
COP_{HP}	Hourly COP of HP [-]
c_p	Specific heat of water (4180) [J/kg K]
d_i	Thickness of insulation of STES [m]
d_{min}	Minimum thickness of insulation [m]
dQ_{int}	Internal energy change in the STES over successive years [Wh]
d_t, d_s,d_b	Thickness of insulation of STES (top, side and bottom, respectively) [m]
$E_{in.boil}$	Primary energy input to boiler [Wh]
$E_{in.el}$	Primary energy input to HP [Wh]
f_{dem} (m)	Factor for modifying heat demand profile for month 'm' [−]
f_{sup} (m)	Factor for modifying heat supply profile for month 'm' [−]
H	Height of STES [m]
K_t, K_s, K_b	Envelope loss coefficient of STES (top, side and bottom, respectively) [$W/m^2 \cdot K$]
m	Month of the year [−]
Q_{amb}	Heat extracted from ambient air [Wh]
Q_{boil}	Heat supplied by boiler [Wh]
$Q_{cut.dis}$	Cut off limit for discharge of STES [Wh]
Q_{dem}	Heat demand [Wh]
$Q_{DH.loss}$	Heat loss in DH system [Wh]
Q_{dir}	Heat supplied directly by RE source to meet heat demand [Wh]
$Q_{dis.sto}$	Total heat supplied by heat storage [Wh]
Q_{el}	Heat supplied by electricity [Wh]
Q_{HE}	Heat extracted from STES and supplied by HE [Wh]
Q_{HP}	Total heat supplied by HP [Wh]
$Q_{in.HP}$	Heat extracted from STES and supplied by heat pump [Wh]
Q_{in}	Heat charged into STES [Wh]
$Q_{initial}$	Heat content in the STES at the commencement of simulation [Wh]
Q_{loss}	Heat loss from STES [Wh]
$\dot{Q}_{max.HP}$	Designed maximum capacity of heat pump [W]
Q_{max}	Maximum heat stored in STES corresponding to designed $T_{max.sto}$ [Wh]
Q_{min}	Minimum heat stored in STES corresponding to designed $T_{min.sto}$ [Wh]
$Q_{req.HP}$	Heat required to be supplied by HP (without any constraints on capacity) [Wh]
$Q_{sto(rtn.DH)}$	Heat content stored in STES, when temperature in store is $T_{rtn.DH}$ [Wh]
Q_{sto}	Heat content stored in STES [Wh]
Q_{sum}	Heat delivered into DH system [Wh]
$Q_{sup.norm}$	Normalised hourly heat supplied [Wh]
$Q_{sup.rep}$ (m)	Reported value of heat supply (month) [Wh]
Q_{sup}	Heat supplied by RE heat source [Wh]
Q_t, Q_s, Q_b	Heat loss from STES (top, side and bottom, respectively) [Wh]
Q_w	Heat wasted [Wh]
R	Radius of STES [m]
S_c	Surface area of the STES in contact with ground [m^2]
S_t, S_s, S_b	Surface area of the STES (top, side and bottom, respectively) [m^2]
T_{amb}	Ambient temperature of air [°C]
$T_{avg.soil}$	Average (yearly) temperature of soil (around the underground STES) [°C]
T_{DH}	Average (yearly) supply (forward) temperature of DH system [°C]
T_{lim}	Designed cut off temperature for water source heat pump [°C]
$T_{max.sto}$	Designed maximum temperature in STES [°C]
$T_{min.sto}$	Designed minimum temperature in STES [°C]
T_{out}	Temperature of water delivered to HE from STES [°C]
T_{ref}	Reference temperature [°C]
$T_{rtn.DH}$	Return temperature of DH system [°C]
T_{sto}	Average temperature in STES [°C]
$T_{top.sto}$	Estimated temperature at top of STES [°C]
T_{water}	Ambient temperature of waste water [°C]
U_m	H/R (Multiplicative factor) [−]
V	Volume of STES [m^3]
η_{boil}, eta_{boil}	Thermal efficiency of boiler [%]
η_{el}, eta_{el}	Efficiency of conversion of PES to electricity [%]
η_{HP}, eta_{HP}	HP efficiency [%]
λ_i	Thermal conductivity of insulation [W/m K]
λ_{soil}	Thermal conductivity of soil [W/m K]
λ_t, λ_s, λ_b	Thermal conductivity of insulation of STES (top, side and bottom, respectively) [W/m K]
ρ	Density of water (1000) [kg/m^3]

2017 [6,7]. TES also helps in lowering installed heating capacity, primary energy consumption and CO_2 emissions by integrating renewables in the energy mix [8,9]. Energy storage technologies contribute to decarbonisation of heating and one can choose between centralised and distributed designs. The stored heat can be subsequently extracted for use in winter and can be distributed by DH systems, thereby replacing heat supply from fossil fuel boilers, ultimately leading to a reduction in CO_2 emissions. Based on a financial analysis of a small STES (23,000 m^3) in Ireland, it was concluded that solar thermal with storage made a better business case than electricity for meeting the heat demand of a single family, low energy demand house [10]. It was also noted that "some

Please cite this article as: K. Narula et al., Simulation method for assessing hourly energy flows in district heating system with seasonal thermal energy storage, Renewable Energy, https://doi.org/10.1016/j.renene.2019.11.121

smaller-scale systems have become cost competitive or nearly competitive in remote communities and off-grid applications and large-scale thermal storage technologies are competitive for meeting heating and cooling demand in many regions" [11]. Hence, water based STES are being implemented across Europe and the major findings from different sites have been summarised in Ref. [12].

TES can be classified on three different principles: sensible heat storage, latent heat storage (e.g. using phase change materials) and thermo-chemical storage (e.g. using chemical reactions to store and release thermal energy) [8]. Sensible heat storage systems – which typically use water or soil as a storage medium – are a proven technology and central solar heating plants with seasonal storage (CSHPSS) have been in operation since 1990s. Some commonly used sensible TES are borehole thermal energy storage (BTES), aquifer thermal energy storage (ATES), water gravel thermal energy storage (WGTES), pit thermal energy storage (PTES) and tank thermal energy storage (TTES) [13]. Germany has several TTES and WGTES, whereas ATES is prevalent in the Netherlands and many BTES are found in Sweden [14–16]. Over the past few years, TES has been used for DH and cooling in many Nordic countries and Denmark has several large scale PTES [17].

STES can be used for an individual household or can be scaled up to meet the heating demand of thousands of households [18]. Large-scale water tanks are installed in approximately 280 DH systems in Denmark [19]. Sensible heat based storages typical exhibit between 50 and 90% thermal efficiency and the cost of heat delivered varies from 0.1 to 10 €/kWh [7]. Although latent TES systems require a smaller volume, the energy storage cost (€/kWh) of these systems is still 1.5–4 times higher than hot-water systems [20]. TTES and PTES have a higher construction cost per unit volume as compared to ATES and BTES [21]. However, the former are capable of providing higher charging/discharging power due to larger operational temperature difference and flowrates [22]. A heat exchanger (HE) is often used to extract the stored heat from the STES, but when HPs are used in addition, the heat store can be discharged to a lower temperature, thereby increasing the recovery of heat from the STES [23,24]. The costs for large-scale PTES have been falling and an investment cost of 20–40 €/m^3 has been realised in Denmark for very large (>100,000 m^3) PTES systems in the last decade [25]. Large scale DH plants coupled with solar heating and STES are envisioned to play an important role in the Danish smart thermal grid for providing 100% RE based heating systems [26].

As seasonal heat storage becomes a cost effective option for decarbonising heat supply, modelling and simulation studies for STES are increasingly being undertaken. Modelling of a large scale STES in DH system follows a hierarchical process of pre-design, detailed design, technology integration, evaluation and optimisation [22]. The process of pre-design is important in order to evaluate the feasibility of the STES. A preliminary assessment of performance is then undertaken based on key performance indicators of the integrated heating system.

Different types of STES have been compared and the existing design tools for modelling STES have been reviewed in Ref. [27]. Some of the simulation programs which have been used for pre-designing heating systems with STES are MINSUN, Solarthermie-2000, and SOLCHIPS [27]. FEFLOW, CONFLOW, and TRNAST are used exclusively to model ATES; EED (Earth Energy Designer), Geostar, Duct Ground Heat Storage (DST) model and SBM (Superposition Borehole Model) are used specifically to model BTES [27]. For other energy system simulation models which are used for a detailed assessment of STES, the reader is referred to Ref. [22].

Different models for heat supply which are integrated with solar collectors, HPs and thermal storage have been developed and analysed in Refs. [28–30]. TRNSYS (Transient system simulation tool) has been used to examine the performance of different configurations having a STES [31–36]. Panno et al. assessed the energy and economic performance of two systems: one using a HP along with a solar assisted BTES and the other using a conventional gas boiler for heating a school building in Italy [37]. TRNSYS was used to model the building heat demand while DST was used to model the BTES. Ref. [38] uses a TRNSYS simulation model to study the performance of solar DH systems with STES in the UK. TRNSYS was used to optimise the size of a solar thermal system and the volume of a STES for a single family house in Greece [39]. Ref. [40] performed a parametric analysis in order to investigate the performance of a centralised hybrid solar DH network integrated with a seasonal BTES using TRNSYS. Ref. [41] reported the results collected over 19 months of operation from an experimental set up where a solar assisted ground source HP was used in combination with a shallow BTES for heating a domestic building. It used TRNSYS to model solar radiation and a numerical model for heat storage in BTES. Ref. [42] compared thermochemical and sensible-heat storage in two cities in Slovenia. The analysis was performed using ANSYS model for microscale applications and TRNSYS for macroscale assessment. Ref. [43] optimised the spatial layout and simulated a distributed control framework to store heat in ATES using a combination of building energy model, groundwater model and an optimisation tool for the city of Utrecht, Netherlands. TRNSYS has also been used for pre-designing and has been integrated with other building simulation tools such as eQuest and HVACSIM + for undertaking detailed design of the heating system [27]. Ref. [44] compared the results for a prototype plant having a solar collector, thermal storage and a HP to provide the heating demand for a representative building in three cities: Rome, Milan and Cracow using Matlab software. The EINSTEIN (effective integration of seasonal thermal energy storage systems in existing buildings) tool, which is also based on TRNSYS simulations, has been applied for examining the feasibility of STES for buildings [45]. A decision support tool has also been developed as a web-based application, which gives detailed results but lacks transparency as it retrieves the results from a stored library [46]. The solar district heating (SDH) tool is another online tool for undertaking a preliminary cost-benefit analysis of STES which is integrated with solar district heating [47]. This examines different pre-defined configurations for centralised or distributed solar heating and allows the user to compare key performance metrics. This tool is also based on detailed TRNSYS simulations results which have been pre-calculated in the model.

While a specialised software can be used for undertaking a detailed simulation, a simple model using energy balances may be equally useful for undertaking a preliminary assessment, saving time and computational effort and being potentially more relevant for pre-design purposes. Following this approach, a simple method for modelling thermal heat storage and simulation of monthly energy flows in a STES has been undertaken in Ref. [48]. The model was validated using TRNSYS and it has been concluded that there are only small variations between the obtained results from both approaches [48]. Ref. [49] also used simple energy balance equations to model the TTES at Friedrichshafen and compared the performance metrics with monitored results. A simple simulation method was proposed and the results were also compared with the monitored data for PTES at Dronninglund (Denmark) [50]. Ref. [49] is a case specific analysis, only assesses the STES and undertakes the assessment on a monthly basis. Ref. [50] undertakes an hourly simulation, but models only the PTES (does not model the entire heating system). Standard key performance indicators such as CO_2 emissions, share of RE, and costs have not been modelled in both these methods and hence cannot be analysed. As highlighted

Please cite this article as: K. Narula et al., Simulation method for assessing hourly energy flows in district heating system with seasonal thermal energy storage, Renewable Energy, https://doi.org/10.1016/j.renene.2019.11.121

above, TRNSYS has been most commonly used for assessment of STES in combination with other tools. However, energy balance equations can also be used as an alternative to examine energy flows in a heating system. To conclude, although there are specific tools for the assessment of a STES, transparent and easy to use generic models for analysing the complete heating system are limited.

This paper presents a simulation method for modelling hourly energy flows in a DH system with a STES. A simple tool has been designed using the proposed method and has been implemented on a spreadsheet. A key contribution of this paper is to model the DH system at an hourly interval in a transparent and an easy to use manner without using a proprietary software. Validation of the method allows us to simulate hourly energy flows in cases where energy flows are not monitored. The tool can also enable us to examine energy flows for identifying feasible operational regimes of different heat sources. The tool is planned to be made publicly available.

Section 2 discusses the theoretical model, tool and configurations of the heating system which can be assessed using the proposed method. While the complete tool is presented, we only show the results which are useful for validating the model for selected configurations in this paper. Section 3 presents the methodology and the data inputs for the assessment. Section 4 presents the simulated energy flows and compares them with the reported results for two of the four configurations in order to validate the model. Section 5 discusses the results before concluding the paper.

2. Model

A deterministic model is developed which is used to simulate hourly energy flows in a DH system. Various configurations of the system with different heating sources and a STES have been considered. Energy balance equations, a set of predetermined conditions and constraints are used for simulating energy flows in the system. The tool has been designed to assess the pre-feasibility of integrating a hot-water STES in a DH system. The model and method can also be used to optimise the operation of different heating sources with the objective of minimising primary energy consumption, energy cost or CO_2 emissions. The framework of the assessment tool is shown in Fig. 1.

2.1. Description of tool

The hourly heat demand for a given set of households is predefined and is fed exogenously into the model. It consists of DHW and SH demand and is a function of the number of households, heat demand characteristics such as hot water consumption per inhabitant and specific SH demand. The latter depends on the number of heating degree days which is a function of the external temperature at the considered location for the specific year, as well as building characteristics and usage. The hourly heat supply is also provided as an exogenous input to the model. This heat supply can be from a renewable source such as geothermal heat, from an incinerator plant operating at its designed capacity, or from an intermittent source such as a solar thermal plant. Other design parameters of the STES, heating equipment and DH system are also set exogenously.

As this is a generic tool, different cases (corresponding to different number of households) can be evaluated. The configurations are predefined and are explained in section 2.2. The model calculates the available excess heat based on the expected heat supply and demand profiles and estimates the STES volume for storing the surplus heat. The optimal dimensions of the STES (e.g. radius, height) to store the estimated water volume are calculated such that the surface area and hence the heat losses are minimised. Thereafter, heat losses are calculated based on the physical characteristics of the STES and its surroundings. The model simulates hourly energy flows in the system and calculates the heat content in the STES from the energy balance. Various parameters such as final energy input from different sources, annualised capital costs, operational costs and CO_2 emissions have been calculated for different configurations. The primary energy supply (PES), share of RE in the system and the required peak load on the electricity grid (from operation of the HP) have also been calculated. The annualised capital costs and the operational cost have been used to calculate the levelised cost of heat supply. Subsequently, key performance indicators for different configurations can be compared as basis for deciding whether to deploy the STES in a DH system.

2.2. Configurations

Four pre-defined configurations can be examined using this tool.

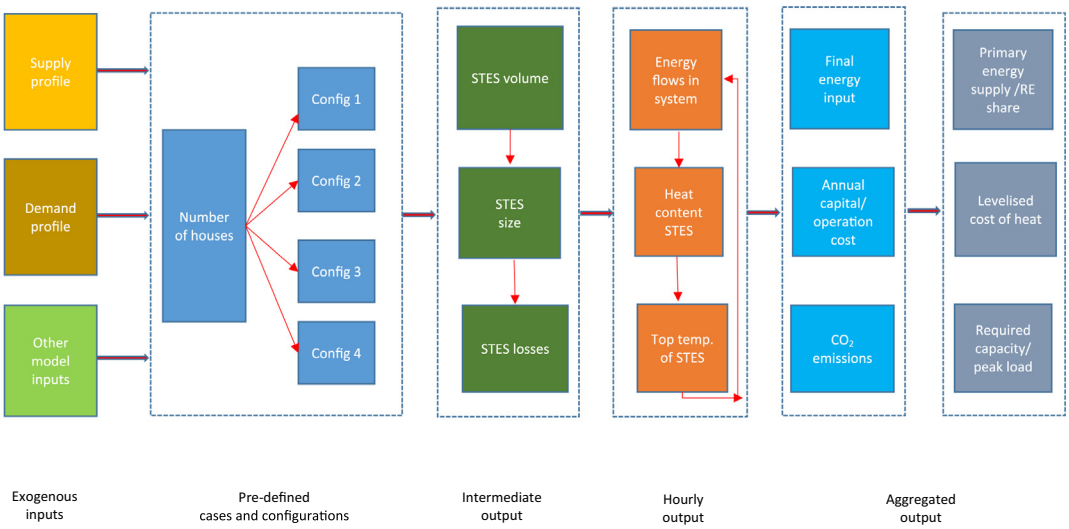

Fig. 1. Framework of the assessment tool.

Please cite this article as: K. Narula et al., Simulation method for assessing hourly energy flows in district heating system with seasonal thermal energy storage, Renewable Energy, https://doi.org/10.1016/j.renene.2019.11.121

- Configuration 1: System with only a boiler (reference configuration)
- Configuration 2: System with a RE source, a boiler, a thermal storage, and a HE
- Configuration 3: System with a RE source, a boiler, a thermal storage, a HE and a HP
- Configuration 4: System with a RE source, a boiler, and a HP (but no storage)

The explanations and the equations for different configurations are given in the following sub-sections. As most equations have the same time instant (t), it is only mentioned explicitly when the time instant are different. It is assumed that the DH system is supplied at an average (annual) supply temperature of T_{DH} and annual variations in T_{DH} have been neglected.

2.2.1. Configuration 1

Fig. 2 shows the heating system with only a boiler.

The centralised boiler meets the entire Q_{dem}. The boiler has to supply Q_{sum} where Q_{sum} is the total heat supplied into the DH system by all energy sources. In this configuration the boiler is the only source of energy and is represented by Equation (1).

$$Q_{boil} = Q_{sum} \quad (1)$$

There is heat loss in the DH system ($Q_{DH.loss}$) and the heat supplied to the DH system is given by Equation (2).

$$Q_{sum} = (Q_{dem} + Q_{DH.loss}) \quad (2)$$

The PES to the boiler can be calculated using Equation (3).

$$E_{in.boil} = Q_{boil} / \eta_{boil} \text{ ('η' is shown as 'eta' in the figure)} \quad (3)$$

2.2.2. Configuration 2

Fig. 3 shows the heating system with a RE source, a boiler, a thermal storage, and a HE.

Heat from RE source is supplied directly to meet the heat demand according to Equation (4).

$$Q_{dir} = \text{MIN}\,[Q_{sum}, Q_{sup}] \quad (4)$$

The model uses the Heaviside step function H (see Fig. 3) to simulate the decision making according to certain predefined conditions. These decisions are physically implemented in the hydraulic system using appropriate control elements. The Heaviside step function H is defined in Equation (5):

$$H(X) = \frac{d}{dx}\text{MAX}\{x, 0\} \text{for } x \neq 0 \quad (5)$$

When the heat demand Q_{sum} is smaller than Q_{sup} the excess supply of heat is routed to the STES, as shown by Equation (6).

$$Q_{in} = \text{MAX}\,[(Q_{sup} - Q_{sum}),0] \cdot [1\text{-}H\,(x' - x)], \text{ where } x' = T_{max.sto} \text{ and } x = T_{sto} \quad (6)$$

The Heaviside step function H ensures that Q_{in} is delivered to the STES when $T_{sto} < T_{max.sto}$ and $Q_{in} = 0$ when $T_{sto} \geq T_{max.sto}$

The limits of water temperature in the STES are shown by Equation (7).

$$T_{max.sto} > T_{sto} > T_{min.sto} \quad (7)$$

The maximum and minimum heat storage capacity of the STES is given by Equation (8).

$$Q_{max} = V \cdot \rho \cdot c_p \cdot (T_{max.sto} - T_{ref});\ Q_{min} = V \cdot \rho \cdot c_p \cdot (T_{min.sto} - T_{ref}) \quad (8)$$

If T_{sto} reaches $T_{max.sto}$, the energy flow into the STES is cut off and excess heat Q_w, is released to ambient. This is represented by Equation (9).

$$Q_w = \text{MAX}\,[(Q_{sup} - Q_{sum}),0] \cdot [H(x' - x)], \text{ where } x' = T_{max.sto} \text{ and } x = T_{sto} \quad (9)$$

When heat demand cannot be satisfied by Q_{dir}, heat is discharged from the STES via the HE. This exchange is possible only if $T_{top.sto}$ is higher than T_{out} (or T_{DH} according to DH system design). The amount of heat supplied from the STES is given by Q_{HE} as shown in Equation (10).

$$Q_{HE} = \text{MIN}\,([Q_{sto} - Q_{min}], [Q_{sum} - Q_{dir}]) \cdot [H(x' - x)], \text{ where } x' = T_{out} \text{ and } x = T_{top\cdot sto} \quad (10)$$

Q_{sum} is supplied into the DH system (given by Equation (2)) and the boiler supplies the balance heat for meeting the demand, shown by Equation (11).

$$Q_{boil} = Q_{sum} - Q_{dir} - Q_{HE} \quad (11)$$

The PES to the boiler can be calculated using Equation (3).

Q_{loss} in the STES are calculated for each hour. The detailed method for calculations of losses for different types of STES is shown in the Appendix. $Q_{sto}(t)$ is initialised at $t = 0$ as $Q_{initial}$ and $Q_{sto}(t+1)$ (in the next hour) can be calculated using Equation (12).

$$Q_{sto}(t+1) = Q_{sto}(t) - Q_{HE}(t) + Q_{in}(t) - Q_{loss}(t) \quad (12)$$

The average temperature in the STES can be calculated as shown in Equation (13).

$$T_{sto}(t+1) = Q_{sto}(t+1) / (V \cdot \rho \cdot c_p) + T_{ref} \quad (13)$$

The temperature at the top of the STES can be calculated from the relationship between $T_{top\cdot sto}$ and Q_{sto} based on the stratification profile in the STES (See section 3.4).

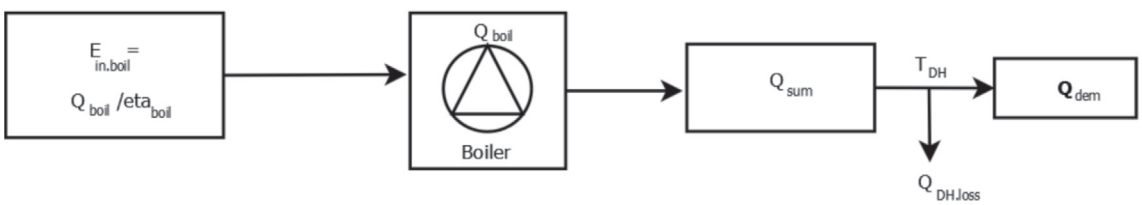

Fig. 2. System with only a boiler (reference configuration).

Please cite this article as: K. Narula et al., Simulation method for assessing hourly energy flows in district heating system with seasonal thermal energy storage, Renewable Energy, https://doi.org/10.1016/j.renene.2019.11.121

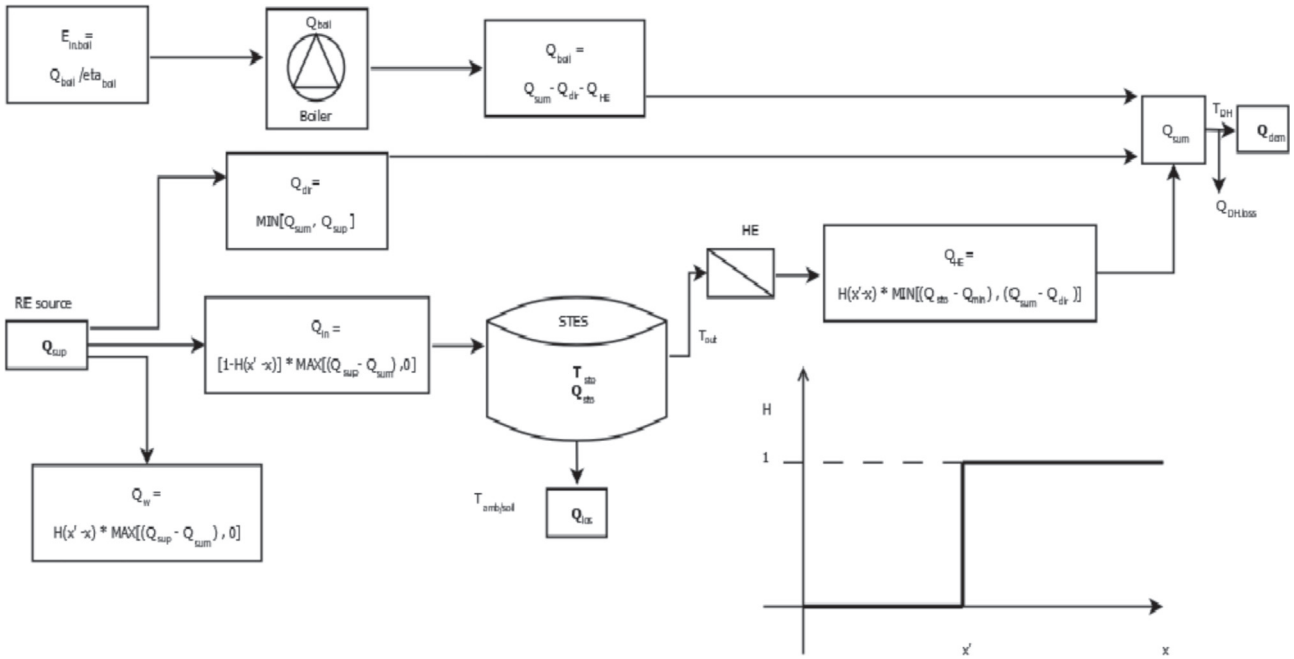

Fig. 3. System with a RE source, a boiler, a thermal storage, and a HE.

2.2.3. Configuration 3

Fig. 4 shows the heating system in configuration 3.

The priority of heat supply is defined in the following order: heat directly from RE source, HE, HP, followed by the boiler. Similar to configuration 2, the STES is discharged through a HE and Q_{dir}, Q_{in}, Q_w, Q_{HE}, T_{sto} and $E_{in.boil}$ are calculated using the same equations as used for configuration 2.

However, when the STES cannot be discharged through the HE (as $T_{top.sto} < T_{out}$), it is used as a heat source for the HP. The required unmet heat demand which could be supplied by the HP is

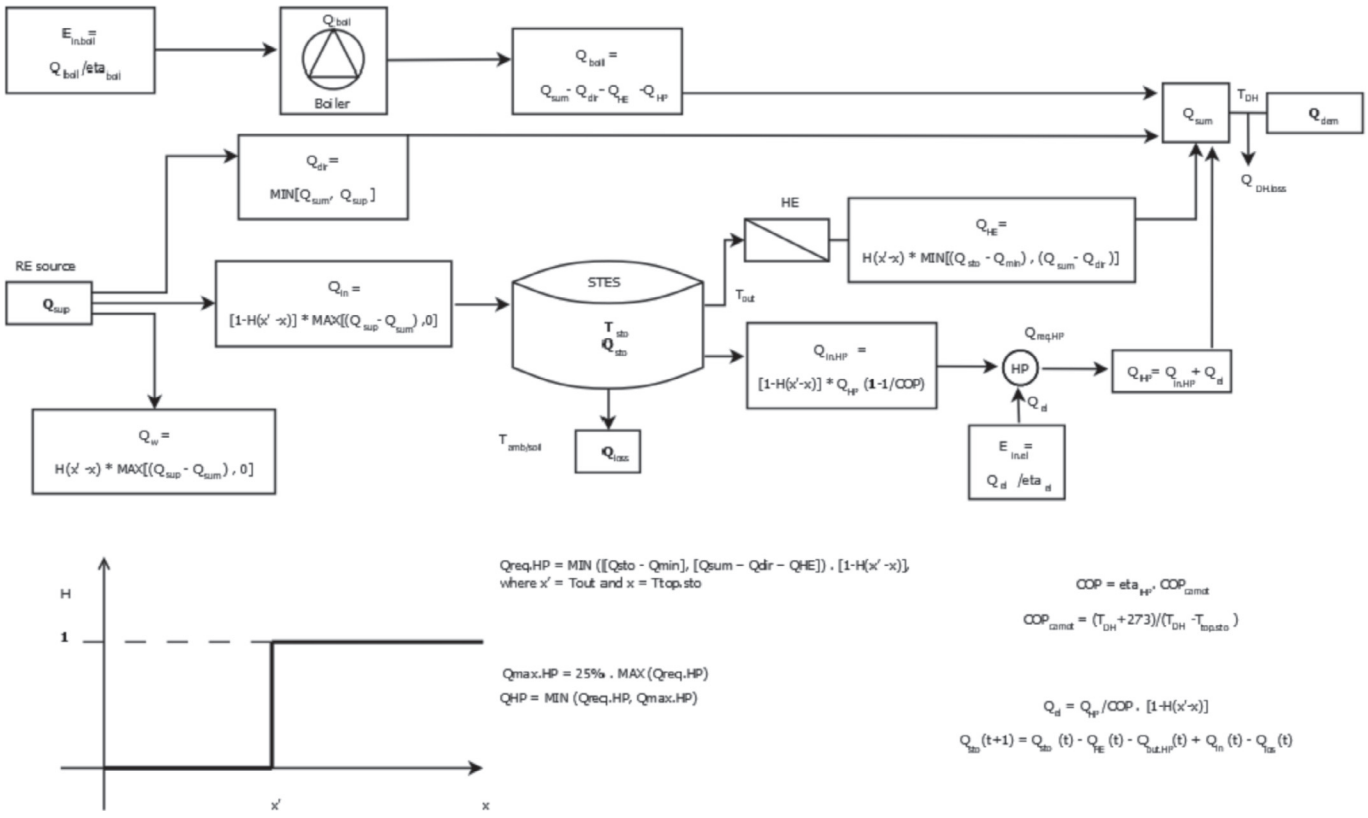

Fig. 4. System with a RE source, a boiler, a thermal storage, a HE and a HP.

Please cite this article as: K. Narula et al., Simulation method for assessing hourly energy flows in district heating system with seasonal thermal energy storage, Renewable Energy, https://doi.org/10.1016/j.renene.2019.11.121

calculated using Equation (14).

$$Q_{req.HP} = MIN\ ([Q_{sto} - Q_{min}], [Q_{sum} - Q_{dir} - Q_{HE}]) \cdot [1\text{-}H(x' - x)], \text{ where } x' = T_{out} \text{ and } x = T_{top\cdot sto} \quad (14)$$

In order to lower the capital cost of the HP and to ensure that it is not oversized, the HP is sized to cover a percentage of the total annual load. Hence the HP provides the majority of the heat demand during the year while the boiler provides the peak load. The selection of the installed capacity of the HP is a design factor and the chosen value for this paper is 25% as shown in Equation (15).

$$Q_{max.HP} = 0.25 \cdot MAX\ (Q_{req\cdot HP}), \text{ where MAX represents the maximum value over the year} \quad (15)$$

The heat supplied by the HP is shown in Equation (16).

$$Q_{HP} = MIN\ (Q_{req.HP}, Q_{max.HP}) \quad (16)$$

The coefficient of performance (COP) of the HP, is given by Equation (17) and η_{HP} is assumed as 50%

$$COP_{HP} = \eta_{HP} \cdot COP_{Carnot} \quad (17)$$

Where the Carnot efficiency (maximal theoretical value) of the HP is given by Equation (18).

$$COP_{Carnot} = [T_{DH}+273] / [T_{DH} - T_{top.sto}] \quad (18)$$

Heat extracted from the STES is shown by Equation (19).

$$Q_{in.HP} = Q_{HP} \cdot (1\text{-}1/COP_{HP}) \cdot [1\text{-}H\ (x' - x)], \text{ where } x' = T_{out} \text{ and } x = T_{top\cdot sto} \quad (19)$$

The electrical energy consumed by the HP is calculated using Equation (20).

$$Q_{el} = (Q_{HP} / COP) \cdot [1\text{-}H\ (x' - x)], \text{ where } x' = T_{out} \text{ and } x = T_{top\cdot sto} \quad (20)$$

The boiler supplies the balance heat which is calculated using Equation (21).

$$Q_{boil} = Q_{sum} - Q_{dir} - Q_{HE} - Q_{HP} \quad (21)$$

Similar to configuration 2, the heat content in the STES can be calculated using Equation (22).

$$Q_{sto}\ (t+1) = Q_{sto}\ (t) - Q_{HE}(t) - Q_{in.HP}(t) + Q_{in}(t) - Q_{loss}(t) \quad (22)$$

Equation (23) is used to calculate the PES from electricity accounting for the efficiency of conversion of primary energy to electricity.

$$E_{in.el} = Q_{el}/\eta_{el} \quad (23)$$

2.2.4. Configuration 4

Fig. 5 shows the heating system in configuration 4 which has a RE source, a boiler and a HP (but no storage).

Similar to configuration 2 and 3, heat from RE source is supplied directly to meet the heat demand according to Equation (4). However, as there is no storage, whenever heat demand is less than heat supply, Q_w is wasted. This is shown by Equation (24).

$$Q_w = MAX\ [(Q_{sup} - Q_{sum}), 0] \quad (24)$$

This heat supply from the RE source is optional as the main source of heat is the HP in this configuration. Ambient heat can be extracted by an electrically operated water–water HP and a waste water treatment plant (temperature 10–20 °C, depending on the season) is chosen as the source of ambient heat.

The heat required to be supplied by the HP can be calculated using Equation (25)

$$Q_{req.HP} = MIN\ ([Q_{sum} - Q_{dir}], 0) \cdot [H(x' - x)], \text{ where } x' = T_{lim} \text{ and } x = T_{water} \quad (25)$$

Similar to configuration 3, there is a constraint on the capacity of the HP ($Q_{max.HP}$) and Equation (15) and Equation (16) are valid. The heat extracted from water from waste treatment plant is shown by Equation (26).

$$Q_{amb} = Q_{HP} \cdot (1\text{-}1 / COP_{HP}) \cdot [H(x' - x)], \text{ where } x' = T_{lim} \text{ and } x = T_{water} \quad (26)$$

Equation (27) gives the maximum theoretical efficiency of the HP

$$COP_{Carnot} = [T_{DH}+273] / [T_{DH} - T_{water}] \quad (27)$$

Similar to configuration 3, the electrical energy consumed by the HP can be calculated using Equation (20) while Equation (17) gives the actual COP of the HP.

$$Q_{el} = (Q_{HP} / COP_{HP}) \cdot [1\text{-}H\ (x' - x)], \text{ where } x' = T_{out} \text{ and } x = T_{water} \quad (28)$$

The boiler supplies the balance heat which is calculated using Equation (29).

$$Q_{boil} = Q_{sum} - Q_{dir} - Q_{HP} \quad (29)$$

Similar to earlier configurations, Equation (3) and Equation (23) are used to calculate the PES from different sources.

3. Methodology

In order to check the validity of the proposed model, the results of the simulation were compared with the reported data for two configurations. The paper selects two real DH systems fitted with solar collectors and a STES for undertaking this comparison: a system with a HE at Friedrichshafen (similar to configuration 2) and a system with a HE and a HP at Marstal (similar to configuration 3). The results are compared for Friedrichshafen in 2002 and for Marstal in 2015 as detailed monitored values are available for these years. Only limited results of the model are reported in this paper.

3.1. DH system description

A solar assisted DH system with a STES was built in Friedrichshafen, Germany in 1996. In the first phase, 2700 m^2 of solar flat plate collectors were mounted on buildings. 23,000 m^2 of floor space was heated (280 apartments in multifamily houses and one kindergarten) and the heating system was equipped with two gas boilers (750 kW and 900 kW). An underground cylindrical tank (reinforced concrete) of 12,000 m^3 was integrated with the system [51]. The STES was equipped with a HE and the hot water extracted from the tank was used to raise the temperature of water to 70 °C to supply it to the DH system for SH. The DHW demand was met by further heating this water at heating substations in the building

Please cite this article as: K. Narula et al., Simulation method for assessing hourly energy flows in district heating system with seasonal thermal energy storage, Renewable Energy, https://doi.org/10.1016/j.renene.2019.11.121

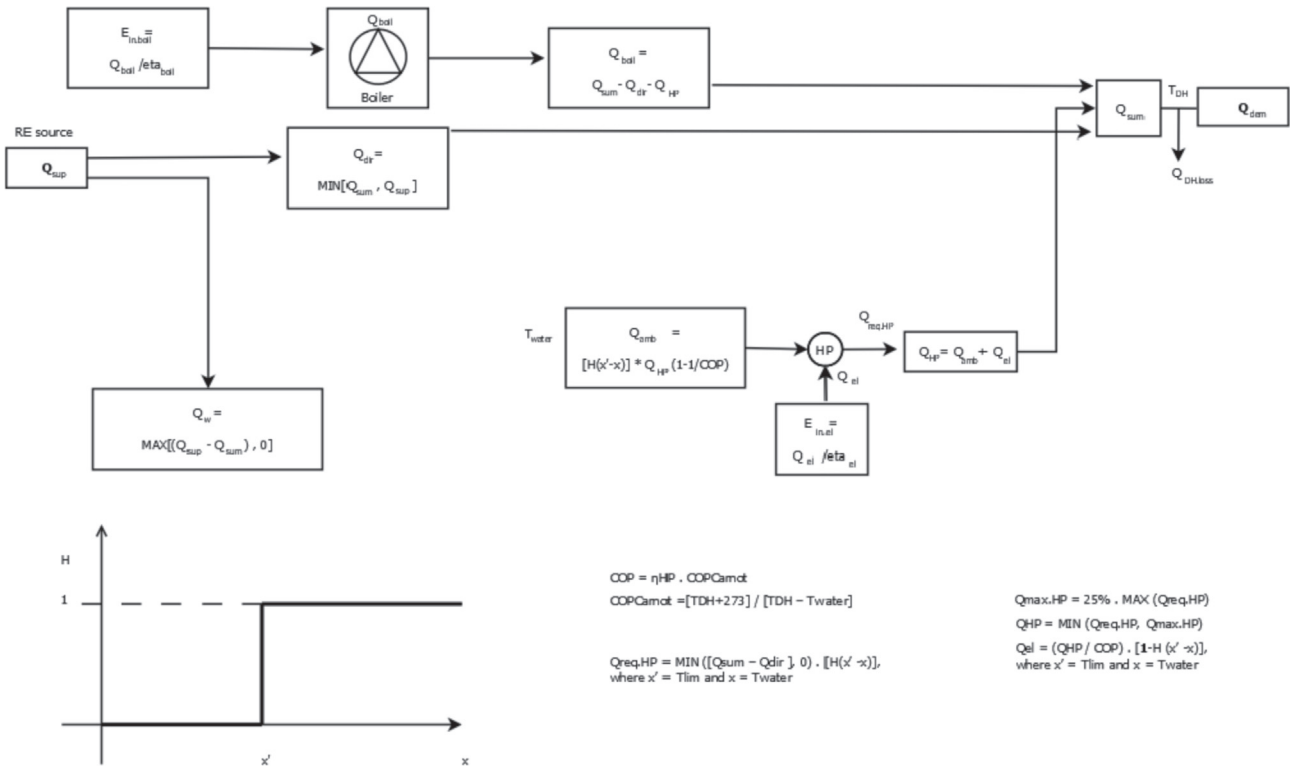

Fig. 5. System with a RE source, a boiler and a HP (but no storage).

[52]. Published reports on heat storage in Germany have been used to provide the input parameters for this study [51–56].

The Marstal DH system is much larger and has a distribution network of about 20 km [57]. It annually supplies around 23 GWh of heat to 1600 consumers with a heated floor area of around 300,000 m^2 [58]. A total of 33,300 m^2 of ground mounted solar collectors provide RE to the system along with an 8.3 MW bio fuel based oil boiler, a 1.5 MW_{th} HP, and a 4 MW_{th} wood chip (biomass) boiler which runs an electricity producing 750 kW_{el} organic Rankine cycle (ORC) unit. As a part of the Sunstore 4 project, a PTES of 75,000 m^3 having a truncated pyramid shape was integrated in the system in 2011–2012 [59]. Energy flows over different years was monitored [60,61] and details about the design and construction of the PTES have been derived from existing literature [62–65].

3.2. Exogenous inputs

The known parameters for Friedrichshafen and Marstal system (see Table 1) are provided exogenously as inputs.

The reported values of thermal conductivity of the thermal insulation and soil and the dimensions of the tank are used to calculate the hourly heat losses for Friedrichshafen. The PTES at Marstal did not have any thermal insulation on the side and bottom and it was only covered with a thin liner to make it watertight [66]. The top cover has three layers of foam insulation (Nomalen 28N) with a total thickness of 240 mm [64]. However, as the values of the effective conductivity of soil and the insulation and the effective thickness of the insulation at the side and bottom of the PTES were not available for Marstal, these values have been assumed based on the observed heat losses for 2014.

The heat content at the beginning of 2002 for Friedrichshafen and 2015 for Marstal is set as $Q_{initial}$ before the commencement of the simulation [60,61]. Thereafter, the model is run in steps of 1 h from time t = 0 for the two selected cases.

3.3. Supply and demand profiles

The heat supply and demand profiles are provided exogenously as inputs. It is important to know hourly values of Q_{sup} and Q_{dem} (profiles), but they may not be monitored or, may be reported on monthly/yearly basis. The hourly heat demand profile could also be simulated. The demand for hot water can be generated from a known profile of per capita hot water consumption, and number of inhabitants. Hourly heat demand can be calculated using the specific heat demand, heated surface area, external temperature and the required temperature inside the apartment. For design purposes, hourly external temperatures of a standard reference year can be taken depending on the climatic zone (e.g. SIA Standard 381/3) [67] and the hourly temperatures in any given year can be expected to be close to the standard year. Similarly, heat supply would be a function of solar irradiation at the considered location, orientation, solar collector area, and its efficiency. An hourly solar supply profile can also be chosen which is representative of heat supply from the installed solar collectors at a given location.

For the assessment undertaken in this paper, hourly heat supply and demand data is not available for the location and the specific year (Friedrichshafen, 2002 & Marstal, 2015). In order to overcome this data limitation, hourly heat supply and heat demand is recreated using normalised hourly solar thermal supply and heat demand profiles (normalised by maximum hourly values) for a generic city in Denmark (Fig. 6). These have been taken from the library of hourly heat supply and demand profiles provided by Energy PLAN [68]. This can be considered as representative of heat demand at locations having similar climate as Denmark. In the same way, heat supply profile from a representative city in Denmark also reflects the solar insolation in similar meteorological conditions. As these are normalised profiles, they can be scaled to recreate the heat demand profile for the specified number of households and heat supply profile for the assessed case.

Please cite this article as: K. Narula et al., Simulation method for assessing hourly energy flows in district heating system with seasonal thermal energy storage, Renewable Energy, https://doi.org/10.1016/j.renene.2019.11.121

Table 1
Input parameters for the simulation.

	Friedrichshafen	References	Marstal	References
Similar to configuration	2	–	3	–
T_{out} [°C]	55.4	[49]	74	[59]
$T_{max.sto}$ [°C]	95	[53]	90	[65]
T_{ref} [°C]	11	[54]	10	[60]
T_{soil} [°C] (just outside tank)	30	[49]	30	[61]
λ_t, λ_s, λ_b [W/m K]	0.6,0.06,0.6	[55]	0.125, 2, 2	Assumed based on [51]
d_t, d_s,d_b [m]	0.3,0.2,0.3	[56]	0.24,0.5,0.5	[64]
λ_{soil} [W/m K]	3	[55]	2	Assumed based on [60]
$Q_{initial}$ [MWh]	468	[54]	4000	[61]
$Q_{cut.dis}$ [%] (as a % of $Q_{initial}$)	110	Assumed for simulation	85	Assumed for simulation
COP_{max}	NA	–	3.28[a]	[60]
$Q_{DH.loss}$ [%]	18.5[b]	[54]	3	Assumed
$Q_{max.HP}$ [MW]	NA	–	0.7	Assumed for simulation
f_{sup}	Monthly (Table 2)	Calculated	Monthly (Table 2)	Calculated
f_{dem}	Monthly (Table 2)	Calculated	Monthly (Table 2)	Calculated
Shape of tank	Cylindrical	[54]	Trapezoid	[63]
Dimensions of tank [m]	Radius:16	[54]	Top: 113 × 88 Bottom: 50 × 25	[63]
Height of tank [m]	20	[54]	16	[63]

[a] Seasonal COP reported over the year was 3.28.
[b] 2423 MWh of heat was delivered to the DH system (incl. second phase of extension). However, the reported heat consumption was 1976 MWh (excl. second phase of extension). To account for this difference, it was assumed that 447 MWH (18.5% of heat delivered in the network) was lost.

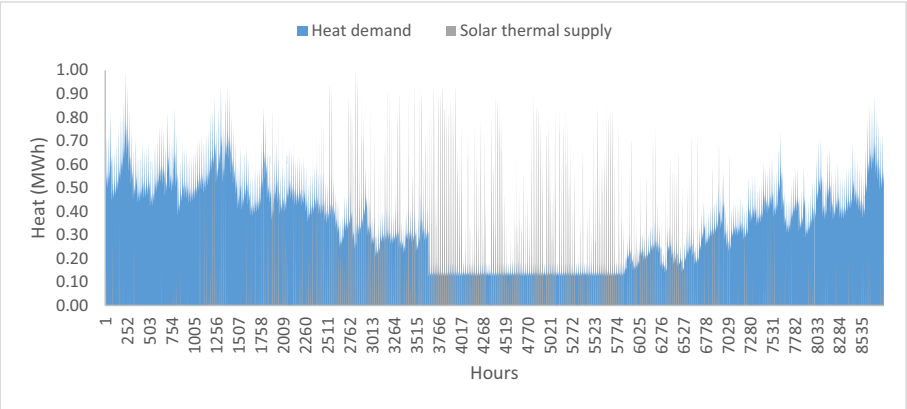

Fig. 6. Normalised hourly heat demand and solar thermal supply profiles.

In order to provide an input to the model, which matches as closely as possible, multiplicative factor, f_{sup} (m) is calculated for every month as shown in Equation (30), where the denominator refers to the normalised hourly supply summed over the specific month.

$$f_{sup}(m) = Q_{sup.rep}(m) / \sum_{h=1}^{720} (Q_{sup.norm}) \quad (30)$$

f_{dem} (m) are also calculated similarly. The hourly normalised supply and demand profiles are then multiplied by the respective monthly factors to obtain the hourly profiles for the month. In the case of Marstal, both the monthly energy supply and demand are reported. However, in the case of Friedrichshafen, monthly demand is not reported. The monthly demand was therefore recreated using the limited data available. The calculated factors are shown in Table 2.

It is acknowledged that although the hourly heat supply and demand of the considered and the actual profile do not match (due to non-availability of meteorological data), but the quantity of monthly (and annual) supply and demand would be same, as they have been equated for calculating the supply and demand factors.

Table 2
Monthly factors for heat demand and heat supply.

Month	Friedrichshafen (2002)		Marstal (2015)	
	f_{dem} (m)	f_{sup} (m)	f_{dem} (m)	f_{sup} (m)
January	0.7	1.7	9.5	19.0
February	0.7	0.6	8.9	13.3
March	0.7	2.2	9.2	32.2
April	0.6	1.5	8.8	24.4
May	0.2	1.6	7.7	17.9
June	0.4	1.5	12.3	14.9
July	0.5	1.4	9.6	18.1
August	0.5	1.2	9.0	17.8
September	0.8	1.4	7.4	20.6
October	0.5	1.3	8.8	15.3
November	0.6	1.1	8.3	11.5
December	0.8	0.3	8.8	4.4
Annual average	**0.6**	**1.4**	**8.9**	**18.7**

3.4. Stratification in STES

Stratification is known to improve the performance of water based TES systems and hence large STES are typically designed as stratified tanks. Various methods for modelling and assessing the

Please cite this article as: K. Narula et al., Simulation method for assessing hourly energy flows in district heating system with seasonal thermal energy storage, Renewable Energy, https://doi.org/10.1016/j.renene.2019.11.121

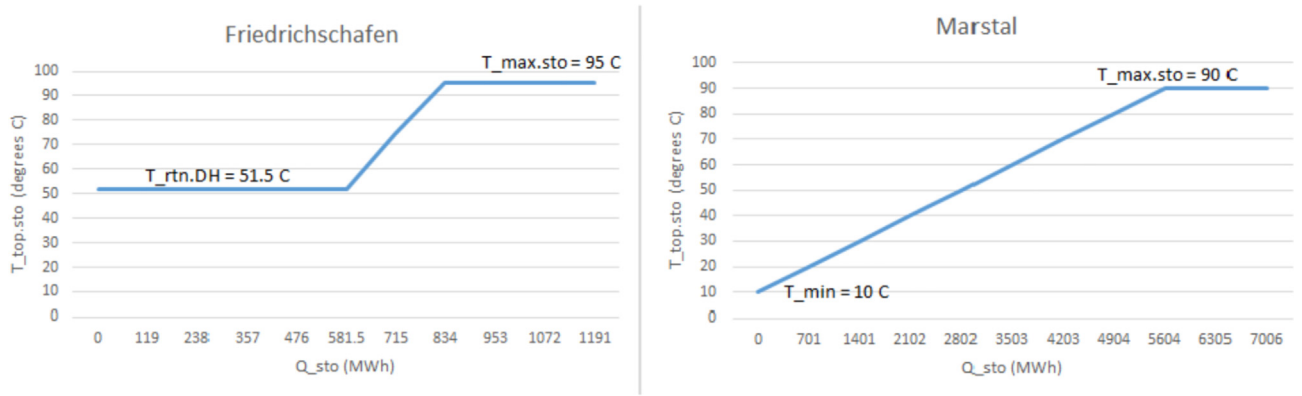

Fig. 7. Stratification model for STES at Friedrichshafen and Marstal.

performance of stratified TES systems have been reviewed in Ref. [69]. Computational fluid dynamics has been used to model stratification in a hot water tank [70] and for PTES at Marstal [71]. As this tool intends to provide a simple simulation method, it uses an expected stratification profile to estimate $T_{top.sto}$ from Q_{sto}. This approximation is considered sufficient as $T_{top.sto}$ is recreated only to identify the condition for operation of the HE and the HP (e.g. if $T_{top.sto} > T_{out}$). The expected stratification profiles in STES with a HE (Friedrichshafen) and in STES with HE and a HP (Marstal) (shown in Fig. 7) are used.

The minimum temperature at the top of the STES in the case of Friedrichshafen is the return temperature of the DH network but the STES at Marstal can be discharged to a minimum temperature of 10 °C using the HP. The temperature at the top of the STES is the maximum design temperature in the STES and it is assumed that this is reached when the heat content in the STES reaches a certain percentage of the maximum heat storage capacity of the STES. Different percentages are chosen for Friedrichshafen (70%) and Marstal (78%) as the latter STES has a much larger capacity and this is in agreement with the observed temperature profiles reported in literature for the two STES [54,61]. A linear stratification profile is used between these two limits. Equation (31) and Equation (32) is used to estimate $T_{top.sto}$ from Q_{sto} for Friedrichshafen and for Marstal respectively.

If $Q_{sto} < Q_{sto(rtn.DH)}$, $T_{top.sto} = T_{rtn.DH}$;

If $Q_{sto} > (0.7 \cdot Q_{max})$, $T_{top.sto} = T_{max.sto}$;

If $(0.7 \cdot Q_{max}) > Q_{sto} > Q_{sto(rtn.DH)}$, $T_{top.sto} = T_{rtn.DH} + slope \cdot (Q_{sto} - Q_{sto(rtn.DH)})$,

where $slope = (T_{max.sto} - T_{rtn.DH}) / (0.7 \cdot Q_{max} - Q_{sto(rtn.DH)})$ (31)

If $Q_{sto} > (0.78 \cdot Q_{max})$, $T_{top.sto} = T_{max.sto}$;

If $(0.78 \cdot Q_{max}) > Q_{sto} > Q_{min}$, $T_{top.sto} = T_{min} + slope \cdot (Q_{sto} - Q_{min})$,

where $slope = (T_{max.sto} - T_{min.sto}) / (0.78 \cdot Q_{max} - Q_{min})$ (32)

3.5. Additional constraints

Certain additional constraints were introduced and these are explained in this section. In order to restrict the discharge of STES, a constraint is introduced in configuration 2 and 3. $Q_{cut.dis}$ represents a cut-off limit for heat discharge from the STES ($Q_{sto} \leq Q_{cut.dis}$) during the discharging cycle. $Q_{cut.dis}$ is pre-defined as a given percentage of $Q_{initial}$ and a 100% value implies that heat discharge is cut off when the heat content in the STES reaches the same value as during the start of the simulation. This ensures that the STES is not over discharged at the end of the year.

It was observed from reported results at Marstal that heat discharge from the STES during the month is controlled. This depends on the availability of heat in the STES and the strategy of operation of the HE/HP. However, in this model, HE and HP are automatically operated at full load if certain conditions are fulfilled. As the duration of operation of the HP is not known, an artificial capacity constraint is introduced in the simulation by limiting the value of $Q_{max.HP}$. The replacement of full load operation of the HP at specific hours by continuous operation of a lower capacity HP is essential to ensure that a limited quantity of heat is discharged from the STES every hour, thereby limiting the heat extracted in the month.

A constraint on the COP of the HP (calculated in Equation (17)) was introduced as COP_{max}. This is essential as the maximum achievable COP of the HP is limited by the technical specifications of the HP and the selected value is mentioned in Table 1. If the temperature lift for the HP is lower than 5 °C [$T_{top.sto} < (T_{DH} - 5)$], the HP cannot be operated (due to lack of suitable refrigerant and poor HP efficiency).

4. Simulation results and model validation

Although the complete model has been explained, only limited simulation results which are useful for validating the model, have been presented. The result of the simulation for two selected heat storages Friedrichshafen (configuration 2) and Marstal (configuration 3) are compared with the results reported in literature to validate the proposed method. Energy flows in configuration 1 and 4 have also been simulated (using the same parameters as for Friedrichshafen) and compared.

4.1. Friedrichshafen

The simulated hourly results for heat supply and heat content in TTES at Friedrichshafen is shown in Fig. 8.

Direct heat supply meets the heat demand when the sun is shining. At other times, the heat demand is met by discharging the STES through the HE, but the boiler provides the majority of heat. The reported and the simulated annual energy flows for 2002 in the Friedrichshafen system are shown in Table 3 along with the difference between them. The difference between the reported and

Please cite this article as: K. Narula et al., Simulation method for assessing hourly energy flows in district heating system with seasonal thermal energy storage, Renewable Energy, https://doi.org/10.1016/j.renene.2019.11.121

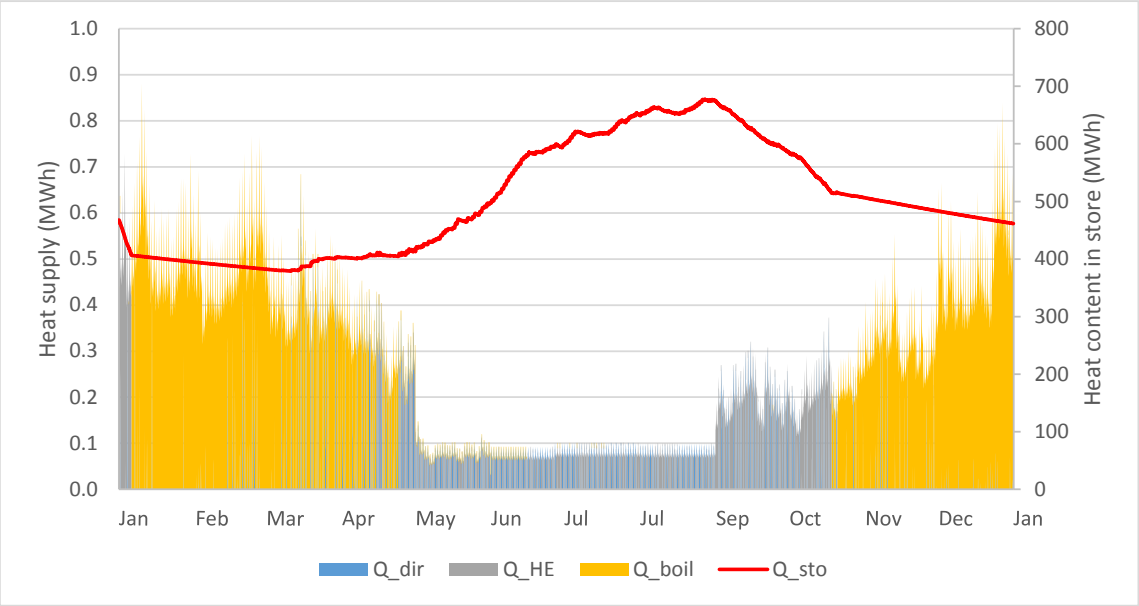

Fig. 8. Simulated hourly results for STES at Friedrichshafen.

Table 3
Reported and simulated annual energy flows for Friedrichshafen system.

Annual values	Reported 2002 [49,54] (A)	Simulated from model (B)	Difference as a % of heat store capacity (A-B)/$Q_{sto.max}$
Q_{sup} (MWh)	989	989	Matched
Q_{dem} (MWh)	1976	1974	Matched
Q_{sum} (MWh)	2423	2340	7%
Q_{in} (MWh)	823	682	12%
Q_{dir} (MWh)	166	307	−12%
Q_{HE} (MWh)	485	393	8%
Q_{boil} (MWh)	1773	1640	11%
Q_{loss} (MWh)	333	295	3%
dQ_{int} (MWh)	4	−6	Less than 1%
Solar fraction (%)	27	30	Less than 1%

the simulated values are shown as a % of the heat storage capacity ($Q_{sto.max}$) of the TTES at Friedrichshafen (normalised by the size of STES).

The solar fraction is calculated using Equation (33).

$$\text{Solar fraction} = (Q_{dir} + Q_{HE}) / Q_{sum} \quad (33)$$

f_{sup} and f_{dem} factors have been selected such that the simulated Q_{sup} and Q_{dem} match with the reported values. The differences in the hourly values of heat supply and demand lead to differences between the annual reported and simulated values of Q_{in}, Q_{dir}, and Q_{HE}. Based on the hourly heat demand, the model simulates that an additional 141 MWh of solar heat is provided directly to meet the demand. Hence, this heat is not routed to the STES thereby showing a corresponding decrease in Q_{in} (reasons discussed in detail later). The observed losses varied between 322 and 360 MWh between 1996 and 2002 [54] and the simulated value of Q_{loss} was 295 MWh.

There are internal energy changes in the STES (dQ_{int}). A negative sign implies that a higher amount of energy is extracted during the year (than what was supplied). Normally a STES is operated such that dQ_{int} is zero but STES can extract larger or smaller quantity of heat over the year resulting in a decrease or increase in heat content of the store respectively, over one cycle of utilisation.

The simulated monthly charging and discharging and the change in energy content of STES at Friedrichshafen is shown in Fig. 9 and this profile closely resembles the reported energy flows shown in Fig. 10 [54].

4.2. Marstal

The simulated hourly results for heat supply and heat content in PTES at Marstal for 2015 is shown in Fig. 11.

There are four sources of heat: direct heat from solar thermal, supplied from PTES through HE, supplied from PTES through HP and boiler. The PTES is operated as a long term storage and completes one cycle of charging and discharging during the year. The storage efficiency is the amount of energy delivered by the STES divided by the total energy supplied to the STES and can be calculated as shown in Equation (34).

$$\text{STES efficiency} = (Q_{HE} + Q_{HP} + dQ_{int}) / Q_{in} \quad (34)$$

Annual energy flows were reported in Refs. [60,61] for Marstal and these are compared with the simulation results in Table 4. This difference is normalised by the size of STES and is reported as a % of heat store capacity.

The reported and simulated results are in good agreement (±10%). The hourly energy flows from the simulation were aggregated to generate monthly heat supply from different sources and these are shown in Fig. 12. These can be compared to the reported

Please cite this article as: K. Narula et al., Simulation method for assessing hourly energy flows in district heating system with seasonal thermal energy storage, Renewable Energy, https://doi.org/10.1016/j.renene.2019.11.121

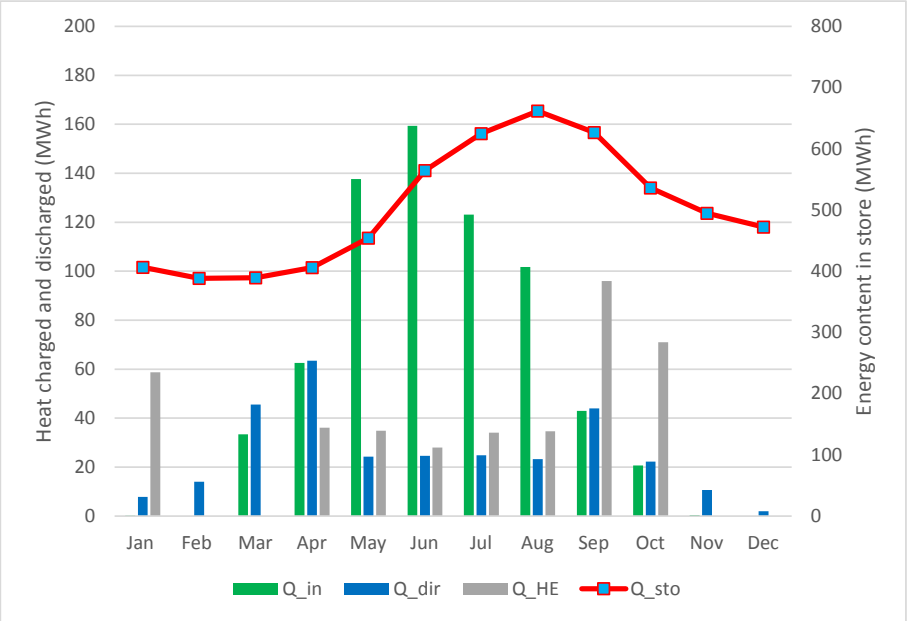

Fig. 9. Simulated charging and discharging of STES at Friedrichshafen.

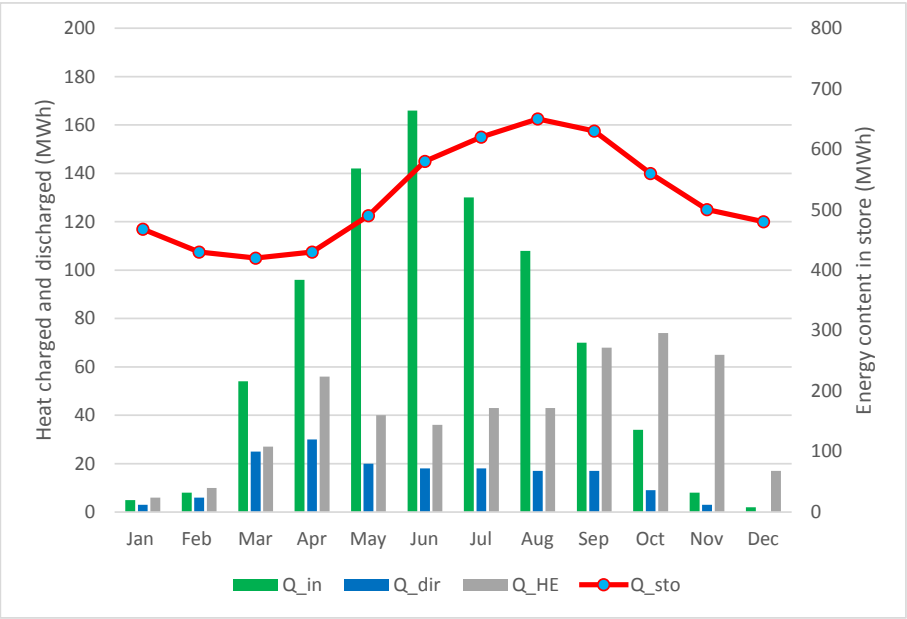

Fig. 10. Reported charging and discharging of STES at Friedrichshafen [data source: 54].

heat supply for 2015 in Fig. 13 [61]. The total energy extracted from the PTES is reported and it is represented as $Q_{dis.sto}$ (sum of Q_{HE} and $Q_{in.HP}$). Q_{boil} refers to the total heat supplied by the two boilers at Marstal.

4.3. Comparison of energy flows in different configurations

The simulated hourly energy flows in configuration 1 and 4 are shown in Fig. 14. The heat demand and supply profiles are kept the same as in the case of configuration 2 at Friedrichshafen.

The annual values for configuration 2 (same as column B in Table 3) are compared with configuration 1 and 4 in Table 5. Although configuration 1 and 4 cannot be validated as these are hypothetical systems, the comparison presents the difference between energy flows in different configurations.

5. Discussion

A summary of the activities undertaken in this study is shown in Table 6.

The reported losses in TTES in Friedrichshafen (333 MWh) were very high compared to the designed loss of 220 MWh [49]. Improper design of the insulation (top and bottom of the tank was not thermally insulated), wet insulation and smaller discharge of heat from the TTES were identified as the main reasons for high losses [31,54].

Please cite this article as: K. Narula et al., Simulation method for assessing hourly energy flows in district heating system with seasonal thermal energy storage, Renewable Energy, https://doi.org/10.1016/j.renene.2019.11.121

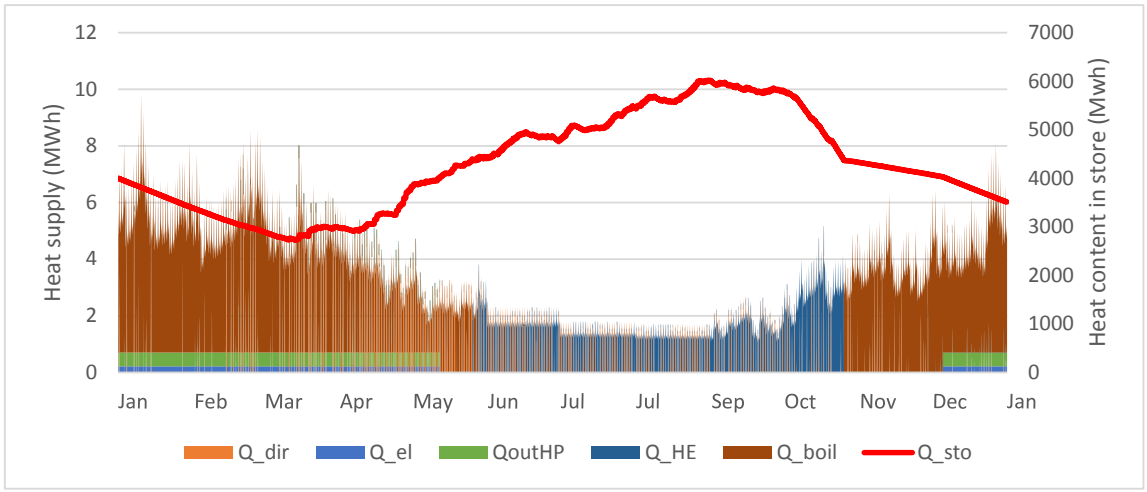

Fig. 11. Simulated hourly results for heat supply and heat content in PTES at Marstal.

Table 4
Reported and simulated annual energy flows for Marstal.

Annual values	Reported 2015 [60,61] (A)	Simulated from model (B)	Difference as a % of heat store capacity (A-B)/$Q_{sto.max}$
Q_{sup} (MWh)	12990	12990	Matched
Q_{dem} (MWh)	27819	27819	Matched
Q_{in} (MWh)	7812	8361	−8%
Q_{dir} (MWh)	5178	4737	6%
Q_{HE} (MWh)	4230	4313	−1%
Q_{HP} (MWh)	1528	1672	−2%
Q_{el} (MWh)	671	733	−1%
Q_{boil} (MWh)	16535	17199	−9%
Q_{loss} (MWh)	2946	2869	1%
dQint (MWh)	−567	−491	−1%
Solar heat delivered (MWh)	10935	10722	3%
Solar fraction (%)	39	39	Less than 1%
Storage efficiency (%)	66.4	65.7	Less than 1%

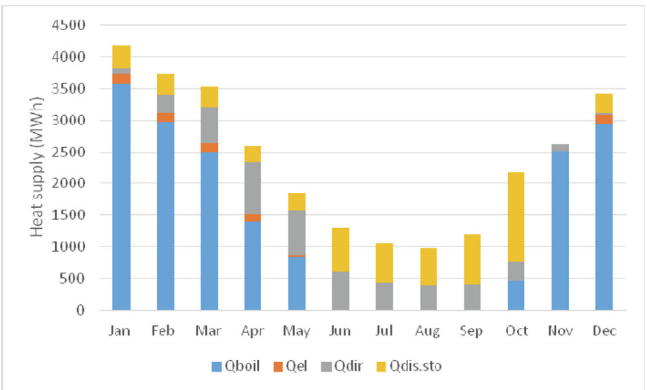

Fig. 12. Simulated monthly heat supply at Marstal.

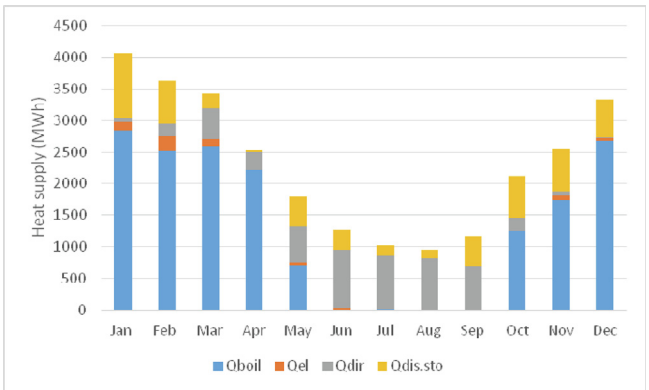

Fig. 13. Reported monthly heat supply at Marstal (2015) [data source: 61].

It is observed that there are some variations in direct use of solar heat, charging, discharging and average heat content of the TTES for each month (compare Figs. 9 and 10). This is due to the difference in hourly heat supply and demand profiles used for the simulation and the actual profiles in 2002 at Friedrichshafen. The hourly heat supply Q_{sup} is a function of solar irradiation at Friedrichshafen in 2002 and this is different from the generic heat supply profile used for this simulation. The generic hourly Q_{dem} used for the simulation is also recreated (as it is not available) from the limited available data and is therefore different from the actual hourly heat demand. Hence, even though the monthly values have been matched by selection of monthly f_{sup} and f_{dem} factors, there is a difference between hourly values. This leads to difference in hourly Q_{dir} and Q_{in} which adds up to monthly and yearly differences. The differences in Q_{in} leads to lower charging of the TTES in the simulation and these daily variations contribute to the differences in Q_{sto} and

Please cite this article as: K. Narula et al., Simulation method for assessing hourly energy flows in district heating system with seasonal thermal energy storage, Renewable Energy, https://doi.org/10.1016/j.renene.2019.11.121

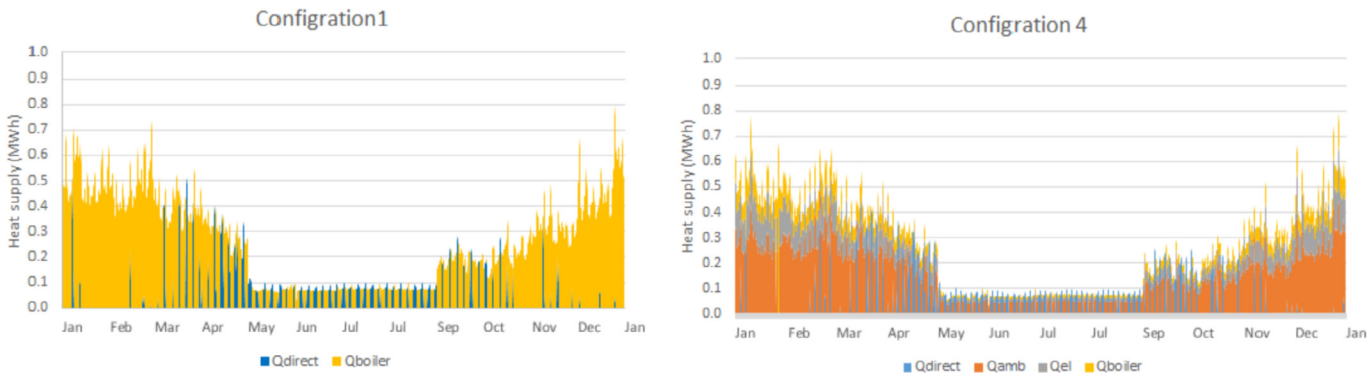

Fig. 14. Simulated energy flows in configuration 1 and 4.

Table 5
Comparison of simulated annual energy flows in different configurations.

Annual simulated values	Config. 2	Config. 1	Config. 4	Comments
Q_{sup} (MWh)	989	989	989	Same supply profile
Q_{dem} (MWh)	1974	1974	1974	Same demand profile
Q_{sum} (MWh)	2340	2340	2340	Same heat delivered to DH system
Q_{in} (MWh)	682	NA	NA	No STES in config. 1&4
Q_{dir} (MWh)	307	307	307	Same heat supplied directly from solar
Q_{HE} (MWh)	393	NA	NA	No HE (with STES) in config. 1&4
Q_{boil} (MWh)	1640	2033	345	Heat supplied by HE & boiler in config. 2 is supplied by boiler alone in config.1
Q_{loss} (MWh)	295	NA	NA	No STES, so no loss in config. 1&4
dQ_{int} (MWh)	−6	NA	NA	No STES, so no change in config. 1&4
Solar fraction (%)	30	13.1	13.1	Heat supplied by solar is stored in config. 2 for supply at a later time
Q_w (MWh)	0	682	682	Solar heat supplied is wasted in config. 1&4 but heat is stored in config. 2[a]
Q_{el} (MWh)	NA	NA	495	Heat is supplied by electricity in config. 4
Q_{amb} (MWh)	NA	NA	1193	Ambient heat is supplied by HP in config. 4

[a] This can however be considered as a hypothetical loss as the solar collectors will be sized such that there is minimum heat wastage.

Table 6
Activities and its components undertaken in this study.

Activities	Components	Location in paper
Overview	Framework of tool	Section 2.1
Modelling	Four configurations	Section 2.2
	Code/algorithm/equations	Section 2.2
	Stratification in STES	Section 3.4
	Additional constraints	Section 3.5
Data inputs for this simulation	Parameters	Section 3.2
	Heat supply/demand profile	Section 3.3
	Assumptions	Table 2
Model validation	Friedrichshafen, 2002 (Configuration 2)	Section 4.1
	Marstal, 2015 (Configuration 3)	Section 4.2
	Only simulation (Configuration 1, 4)	Section 4.3

subsequently to the estimation of $T_{top.sto}$. As the HE operates only if $T_{top.sto}$ is greater than T_{out}, Q_{HE} and consequently Q_{boil} are different for reported and simulated cases. This monthly mismatch is however not particularly concerning as the simulation uses a generic supply profile. In practice, the hourly heat supply and demand profiles in different years are expected to be different from the designed values and while small variations in hourly profiles may lead to monthly differences, they are unlikely to impact average usage of the STES.

In order to observe the impact of using different demand profiles on the results of the simulations, a sensitivity analysis was undertaken using the case of Friedrichshafen. All parameters were kept unchanged but a different demand profile was used for the simulation. A new demand profile (Q_{dem}) was created where the heat demand was kept constant over the entire month. Demand factors were then calculated for different months using the reported energy demand for the month using the procedure mentioned earlier. The percentage difference (median) between the hourly heat demand using the old and the new profiles was observed to be 21%. The simulation was then run using the new demand profile and the results were recorded. It was observed that the variation between the reported and simulated values of Q_{in} and Q_{dir} increased from 12% (shown in Table 3) to 20%. This clearly demonstrates that a variation (between actual and used profiles) of hourly heat demand impacts the simulation of energy flows in the model. A similar result was observed by changing the supply profile. Hence, it can be concluded that the difference in the reported and simulated results are partly due to the unknown heat demand

Please cite this article as: K. Narula et al., Simulation method for assessing hourly energy flows in district heating system with seasonal thermal energy storage, Renewable Energy, https://doi.org/10.1016/j.renene.2019.11.121

and supply profiles.

The maximum temperature at which water could be stored in the tank was 95 °C and hence the heat storage capacity of the tank in Friedrichshafen was 1176 MWh corresponding to a maximum temperature difference of 84 K (T_{ref} = 11 °C). The system was designed so that the minimum temperature to which the TTES could be discharged would be 40 °C (limited by the $T_{rtn.DH}$). Hence, 406 MWh of heat input (corresponding to heat stored in 29 K water) could not be extracted by design (36.5% of heat storage capacity) as the system did not have a HP. This is also referred to as the unusable heat content of the store [54].

The STES in Friedrichshafen was designed to provide about 770 MWh of heat corresponding to a temperature difference of 55 K. However, it was also reported that the average $T_{rtn.DH}$ over the year was 51.5 °C and T_{out} was 55.4 °C. As the return temperature of the DH could not be lowered further due to operational issues at the building level, a further 215 MWh of heat (corresponding to heat stored in 15.4 K of water) could not be extracted from the TTES. Hence a total of 622 MWh heat was 'locked' in the TTES. On the other hand, this unusable heat contributed to heat losses throughout the year. Therefore, absence of a HP and high $T_{rtn.DH}$ were main barriers to the effective utilisation of the TTES at Friedrichshafen.

In the case of Marstal also, the difference between the annual reported and simulated values of Q_{in} and Q_{dir} is attributed to differences between actual heat supply and demand profiles and those used for simulation. This explains the observed differences for Q_{dir}, in Figs. 12 and 13. As Q_{dir} is lower in the simulation results, a higher amount of heat is extracted from the STES by the HE in the summer months. Further, the PTES is discharged to a higher level, which explains the higher difference in the internal energy change.

Secondly, comparison of Figs. 12 and 13 for Marstal reveals that according to the simulation, a large share of the heat could be supplied from the STES in October. This is because extraction of heat from the PTES, (using a HE/HP) is prioritised over the use of boiler in the model. In contrast, reported data shows that the boiler is used to supply a larger share of heat in October. This higher preference for the boiler can be attributed to the operational strategy of the system operators. A possible reason is that boilers may be preffered for heat generation when electricity prices are high, as the biomass boiler at Marstal is connected to an electricity generating ORC unit. In the subsequent months from November to February, the model simulates that a lower amount of heat is discharged from the PTES as it has already discharged most of its heat in October. In contrast, it is observed from the reported results that heat from the PTES is discharged slowly over many winter months. It can thus be inferred that the HP is used selectively to discharge the PTES. The heat supplied by the HP in Fig. 11 does not recreate the actual heat supplied by the HP in the system as it has been artificially constrained by limiting the capacity of the HP to 0.7 MW in the simulation run. In actual practice, the HP is operated to its designed capacity of 1.5 MW_{th} but only during selected hours as decided by the system operators. To conclude, the simulated results cannot recreate the monthly heat supplied from the HP unless the time of operation of the HP is known. However, the model can be used to evaluate the maximum amount of heat which can be extracted from the PTES using the HP over the year. Another advantage of this hourly model is that it could be used to design strategies for the utilisation of the HP with the objective of minimising the cost of electricity for the HP or CO_2 emissions. This would however require additional data, e.g. on the electricity tariff and hourly CO_2 emission factors.

Thirdly, the maximum energy content which can be stored in the PTES at Marstal is around 7000 MWh for a designed maximum (90 °C) and minimum temperature (10 °C). However, it is observed that the PTES is neither charged nor discharged fully. Hence, there is a possibility of better utilisation of the thermal storage capacity which could further lower the use of boilers.

Lastly, T_{DH} was reported to be between 72 and 74 °C for Marstal. Lowering of T_{DH} would lead to higher utilisation of the HE and heat stored in the PTES could be discharged without using the HP, which would eventually save electricity. Consequently, lowering of T_{DH} is an important measure for effective utilisation of the PTES. However, it calls for significant lowering of specific heat demand by retrofitting of buildings as well as delinking supply of DHW through the DH network.

6. Conclusion

The paper presented a simulation method for modelling hourly energy flows in DH systems with STES. In order to validate the method, the results of the simulation of energy flows for two selected cases, Friedrichshafen and Marstal, were compared with values reported in literature. Based on this comparison, the paper concludes that while monthly replication of energy flows in the system depends on the accuracy of inputs, annual energy flows can be closely replicated. The simulated values are in good agreement of the reported values and hence the method can be regarded as validated. Further, if the correct supply and demand profiles, parameters and the operational strategies are provided as inputs to the model, energy flows in the system can be simulated close to the actual values.

The proposed model and the simulation method is simple and reproducible. The tool provides an easy alternative for undertaking a preliminary assessment of the DH system without using a specialised software. While it cannot replace the detailed results offered by complex simulation softwares, this tool can be easily used to simulate hourly energy flows in a DH system thereby giving insights into the operation of the heating system. Unlike models which undertake a monthly or annual assessment, this hourly energy flow model can be utilized to optimise the operation of different energy sources in a multi energy heating system for minimising emissions or total cost of heating and is hence an important contribution to the existing modelling tools. The tool has various other functionalities which have not been presented in detail as the paper intends to present the modelling and related methodological aspects. For example, the tool can be used to estimate the size of the heat storage which would be required for a given heat supply and heat demand profile, hence allowing to assess the capital cost and the feasibility of different configurations. The full exploitation of the tool will be addressed in a subsequent paper.

CRediT author statement

Kapil Narula: Methodology, Software, Validation, Writing - Original Draft, Visualization. Fleury de Oliveira Filho: Methodology, Formal analysis, Writing - Review & Editing. Willy Villasmil: Investigation, Resources, Writing - Review & Editing. Martin K. Patel: Conceptualization, Supervision, Project administration, Funding acquisition.

Declaration of competing interest

The authors declare that they have no known competing financial interests or personal relationships that could have

Please cite this article as: K. Narula et al., Simulation method for assessing hourly energy flows in district heating system with seasonal thermal energy storage, Renewable Energy, https://doi.org/10.1016/j.renene.2019.11.121

appeared to influence the work reported in this paper.

Acknowledgements

This research was conducted in the context of the Swiss Competence Center for Research in Energy, Society and Transition (SCCER-CREST/Contract no. 1155002547), Swiss Competence Center for Energy Research on the Future Energy Efficient Buildings & Districts (SCCER-FEEB&D/Contract no. 1155002547) and Swiss Competence Center for Energy Research on Heat and Electricity Storage (SCCER-HaE Storage/Contract no. 1155002547). All competence centers are financially supported by the Swiss Innovation Agency Innosuisse. This research was also co-funded by Services Industriels de Genève (SIG/Contract no. S19161).

Appendix

Calculation of heat loss from STES

Heat losses can be calculated for different types of STES from the physical dimensions of the heat store and other characteristics. These detailed equations for calculating heat loss in a STES are given ahead [72]. Refer to the nomenclature for details. The specific values used are shown in Table 1.

Cylindrical TTES placed over the ground (Fig. 15)

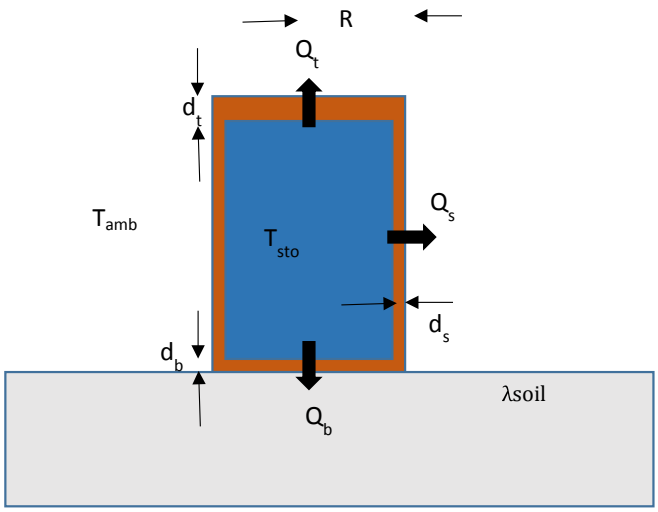

Fig. 15. Dimensions of cylindrical TTES placed over the ground.

Losses from top: $Q_t = (T_{sto} - T_{amb}).\ K_t.S_t$ (35)

Losses from side: $Q_s = (T_{sto} - T_{amb}).\ K_s.S_s$ (36)

Losses from bottom: $Q_b = (T_{sto} - T_{amb}).\ K_b.S_b$ (37)

$$K_t = \frac{\lambda_t}{d_t}\ ;$$

$$K_s = \frac{\lambda_s}{d_s}\ ;$$

$$K_b = \left(\frac{d_b}{\lambda_b} + \frac{4.R}{3.\pi.\ \lambda_{soil}}\right)^{-1} \text{ if } d_b > 0.2\ .\ R \cdot \frac{\lambda_b}{\lambda_{soil}} \quad (38)$$

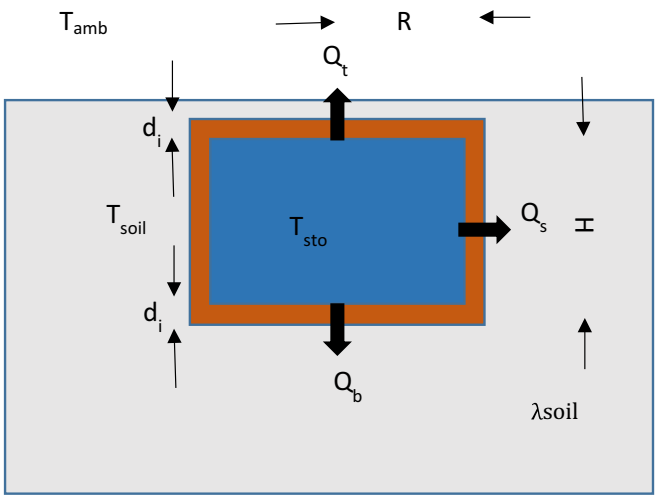

Fig. 16. Dimensions of cylindrical TTES placed underground.

Cylindrical TTES placed underground (Fig. 16)

Losses from top: Same as Equation (35) and K_t is given by Equation (38).

Losses from side and bottom:

$$Q_s + Q_b = (T_{sto} - T_{soil})\ K_{sb}.S_c \quad (39)$$

Where

$$K_{sb} = \left(\frac{d_i}{\lambda_i} + \frac{U_m.R}{\lambda_{soil}}\right)^{-1} \text{ if } d_i > 2\ .\ d_{min} \quad (40)$$

$$U_m = 0.52 \text{ when } H/R = 1 \quad (41)$$

$$d_{min} = \frac{\lambda_i}{\lambda_{soil}}\ .\ R.\ (0.37) \text{ when } H/R = 1 \quad (42)$$

$$S_c = (\pi\ R.R\ +\ 2\pi.\ R.H) \quad (43)$$

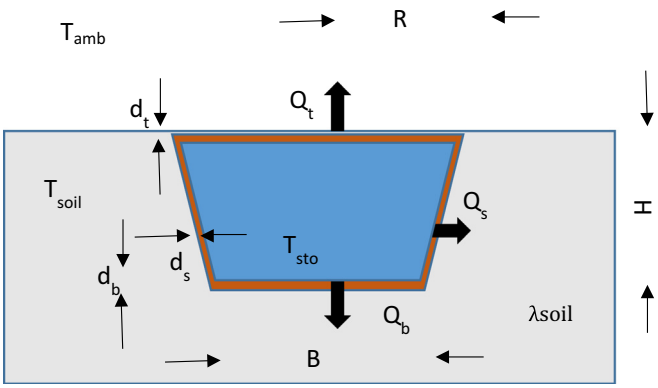

Fig. 17. Dimensions of truncated cone and truncated trapezoid PTES.

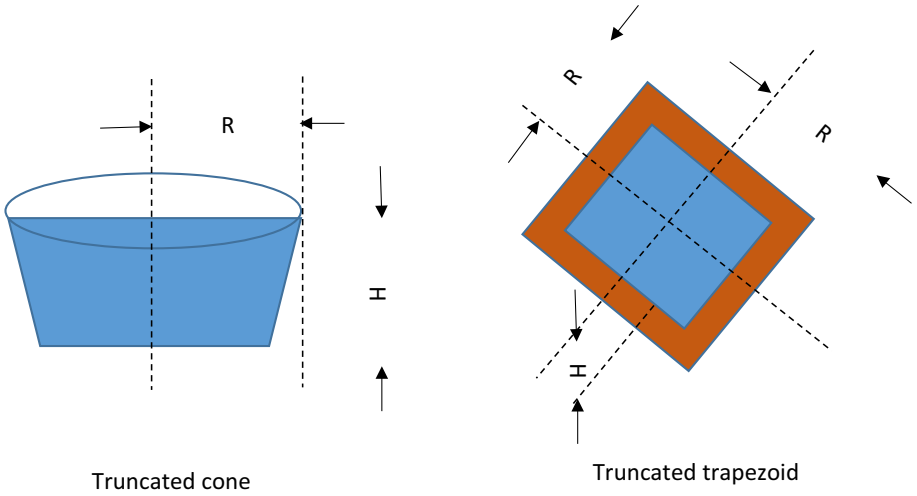

Fig. 18. Dimensions and shape of truncated cone and trapezoid.

Truncated cone and truncated trapezoid PTES (Figs. 17 and 18)

Losses from top: Same as Equation (35) and K_t is given by Equation (38).

$$\text{Losses from side: } Q_s = (T_{sto} - T_{soil}).\ K_s.S_s \tag{44}$$

Where

$$K_s = \frac{1}{b.h} \cdot ln\ \left(\frac{a + b.H}{a}\right) \tag{45}$$

$$b = \frac{\pi}{\lambda_{soil}} \text{ and } a = \left(\frac{d_s}{\lambda_s} + \frac{\pi.H}{2.\ \lambda_{soil}}\right) \tag{46}$$

$$\text{Losses from bottom: } Q_b = (T_{sto} - T_{soil}).\ K_b.S_b \tag{47}$$

Where

$$K_b = \frac{1}{2.b.B} ln\ \left(\frac{c + b.B}{c}\right) \tag{48}$$

$$b = \frac{\pi}{\lambda_{soil}} \text{ and } c = \left(\frac{d_b}{\lambda_b} + \frac{\pi.H}{2.\ \lambda_{soil}}\right) \tag{49}$$

References

[1] OECD/IEA, Transition to Sustainable Buildings. Strategies and Opportunities to 2050, 2013, p. 31. https://www.iea.org/publications/freepublications/publication/Building2013_free.pdf.
[2] Eurostat, Energy consumption in households, 2018 (EU-28, 2016 data), https://ec.europa.eu/eurostat/statistics-explained/index.php/Energy_consumption_in_households [accessed 21 March 2019].
[3] OECD/IEA, Heating in buildings. Tracking clean energy progress, 2018. http://www.iea.org/tcep/buildings/heating/. (Accessed 11 January 2019).
[4] Report of the Conference of the Parties on its twenty-first session, held in Paris from 30 November to 13 December 2015.- decisions adopted by the Conference of the Parties. https://unfccc.int/resource/docs/2015/cop21/eng/10a01.pdf [accessed 10 November 2018].
[5] A.B. Gallo, J.R. Simões-Moreira, H.K.M. Costa, M.M. Santos, E. Moutinho, Energy storage in the energy transition context: a technology review, Renew. Sustain. Energy Rev. 65 (2016) 800–822, https://doi.org/10.1016/j.rser.2016.07.028.
[6] PlanEnergi, Teknologisk Institut, GEO & Grøn Energi, Udredning vedrørende varmelagringsteknologier og store varmepumper til brug i fjernvarmesystemer, 2013. https://ens.dk/sites/ens.dk/files/Forskning_og_udvikling/udredning_om_varmelagringsteknologier_og_store_varmepumper_i_fjernvarmesystemet_nov_2013.pdf.
[7] IRENA, Electricity Storage and Renewables: Costs and Markets to 2030, International Renewable Energy Agency, Abu Dhabi, 2017, p. 13. https://www.irena.org/-/media/Files/IRENA/Agency/Publication/2017/Oct/IRENA_Electricity_Storage_Costs_2017.pdf.
[8] IEA-ETSAP (Energy Technology Systems Analysis Programme) and IRENA, Thermal Energy Storage, Technology Brief E17, Bonn, Germany, 2013.
[9] S. Paiho, H. Hoang, M. Hukkalainen, Energy and emission analyses of solar assisted local energy solutions with seasonal heat storage in a Finnish case district, Renew. Energy 107 (2017) 147–155, https://doi.org/10.1016/j.renene.2017.02.003.
[10] S. Colclough, P. Grif, Financial analysis of an installed small scale seasonal thermal energy store, 86, 2016, pp. 422–428, https://doi.org/10.1016/j.renene.2015.08.032.
[11] OECD/IEA, Energy storage technology Roadmap, 2014. https://www.iea.org/publications/freepublications/publication/TechnologyRoadmapEnergystorage.pdf.
[12] C. Bott, I. Dressel, P. Bayer, State-of-technology review of water-based closed seasonal thermal energy storage systems, Renew. Sustain. Energy Rev. 113 (January) (2019) 109241, https://doi.org/10.1016/j.rser.2019.06.048.
[13] D. Mangold, L. Deschaintre, Task 45 Large Systems Seasonal thermal energy storage Report on state of the art and necessary further R + D, 2015. http://task45.iea-shc.org/data/sites/1/publications/IEA_SHC_Task45_B_Report.pdf.
[14] M. Lundh, J. Dalenba, Swedish solar heated residential area with seasonal storage in rock : Initial evaluation, 33, 2008, pp. 703–711, https://doi.org/10.1016/j.renene.2007.03.024.
[15] P. Fleuchaus, B. Godschalk, I. Stober, P. Blum, Worldwide application of aquifer thermal energy storage – a review, Renew. Sustain. Energy Rev. 94 (April) (2018) 861–876, https://doi.org/10.1016/j.rser.2018.06.057.
[16] E. Nilsson, P. Rohdin, Performance evaluation of an industrial borehole thermal energy storage (BTES) project e Experiences from the first seven years of operation, Renew. Energy 143 (2019) 1022–1034, https://doi.org/10.1016/j.renene.2019.05.020.
[17] H. Gadd, S. Werner, Thermal Energy Storage Systems for District Heating and Cooling. Advances in Thermal Energy Storage Systems: Methods and Applications, Woodhead Publishing Limited, 2015, https://doi.org/10.1533/9781782420965.4.467.
[18] L. Navarro, A. De Gracia, S. Colclough, M. Browne, S.J. Mccormack, P. Grif, L.F. Cabeza, Thermal energy storage in building integrated thermal systems : a review . Part 1 . active storage systems, 88, 2016, https://doi.org/10.1016/j.renene.2015.11.040.
[19] Danish Energy Agency, Technology data for energy storage, Copenhagen, 2019, p. 55, https://ens.dk/sites/ens.dk/files/Analyser/technology_data_catalogue_for_energy_storage.pdf.
[20] J.F. Castro Flores, A.R. Espagnet, J.N.W. Chiu, V. Martin, B. Lacarrière, Techno-economic assessment of active latent heat thermal energy storage systems with low-temperature district heating, Int. J. Sustain. Energy Plan. Manag. 13 (2017) 5–18, https://doi.org/10.5278/ijsepm.2017.13.2.
[21] D. Sveinbjörnsson, L.L. Jensen, D. Trier, I.B. Hassine, X. Jobard, Fifth Generation, Low Temperature, High Exergy District Heating and Cooling Networks (FLEXYNETS), D2.3 Large Storage Systems for DHC Networks, 2017, p. 28. http://www.flexynets.eu/Download?id=file:53241100&s=4576135814681670735.
[22] A. Dahash, F. Ochs, M.B. Janetti, W. Streicher, Advances in seasonal thermal energy storage for solar district heating applications: a critical review on large-scale hot-water tank and pit thermal energy storage systems, Appl. Energy 239 (2019) 296–315, https://doi.org/10.1016/j.apenergy.2019.01.189.
[23] G.K. Pavlov, B.W. Olesen, G.K. Pavlov, B.W. Olesen, Thermal Energy Storage — A Review of Concepts and Systems for Heating and Cooling Applications in Buildings : Part 1 — Seasonal Storage in the Ground, vol. 9669, 2012,

Please cite this article as: K. Narula et al., Simulation method for assessing hourly energy flows in district heating system with seasonal thermal energy storage, Renewable Energy, https://doi.org/10.1016/j.renene.2019.11.121

pp. 515–538. https://www.tandfonline.com/doi/full/10.1080/10789669.2012.667039?.
[24] Z. Wang, F. Wang, Z. Ma, W. Lin, H. Ren, Investigation on the feasibility and performance of transcritical CO_2 heat pump integrated with thermal energy storage for space heating, Renew. Energy 134 (2019) 496–508, https://doi.org/10.1016/j.renene.2018.11.035.
[25] T. Pauschinger, T. Schmidt, P.A. Soerensen, A. Snijders, R. Djebbar, R. Boulter, J. Thornton, Integrated cost-effective large-scale thermal energy storage for smart district heating and cooling. Design aspects for large-scale Aquifer and pit thermal energy storage for district heating and cooling, in: International Energy Agency Technology Collaboration Programme on District Heating and Cooling Including Combined Heat and Power (IEA DHC), 2018. https://www.iea-dhc.org/fileadmin/documents/Annex_XII/IEA_DHC_AXII_Design_Aspects_for_Large_Scale_ATES_PTES_draft.pdf.
[26] Z. Tian, S. Zhang, J. Deng, J. Fan, J. Huang, W. Kong, S. Furbo, Large-scale solar district heating plants in Danish smart thermal grid: developments and recent trends, Energy Convers. Manag. 189 (1 June 2019) 67–80, https://doi.org/10.1016/j.enconman.2019.03.071.
[27] A. Hesaraki, S. Holmberg, F. Haghighat, Seasonal thermal energy storage with heat pumps and low temperatures in building projects — a comparative review, Renew. Sustain. Energy Rev. 43 (2015) 1199–1213, https://doi.org/10.1016/j.rser.2014.12.002.
[28] P.D. Lund, Computational simulation of district solar heating systems with seasonal thermal energy storage, Sol. Energy 36 (5) (1986) 397–408, https://doi.org/10.1016/0038-092X(86)90087-3.
[29] H. Tanaka, T. Tomita, M. Okumiya, Feasibility study of a district energy system with seasonal water thermal storage, Sol. Energy 69 (6) (2000) 535–547, https://doi.org/10.1016/S0038-092X(00)00122-5.
[30] D. Bauer, R. Marx, J. Nußbicker-Lux, F. Ochs, W. Heidemann, H. Müller-Steinhagen, German central solar heating plants with seasonal heat storage, Sol. Energy 84 (4) (2010) 612–623, https://doi.org/10.1016/j.solener.2009.05.013.
[31] M. Reuss, M. Beck, J.P. Müller, Design of a seasonal thermal energy storage in the ground, Sol. Energy 59 (4–6) (1997) 247–257, https://doi.org/10.1016/S0038-092X(97)00011-X.
[32] R. Marx, D. Bauer, H. Drueck, Energy efficient integration of heat pumps into solar district heating systems with seasonal thermal energy storage, Energy Procedia 57 (2014) 2706–2715, https://doi.org/10.1016/j.egypro.2014.10.302.
[33] C.N. Antoniadis, G. Martinopoulos, Simulation of solar thermal systems with seasonal storage operation for residential scale Applications, Procedia Environ. Sci. 38 (2017) 405–412, https://doi.org/10.1016/j.proenv.2017.03.124.
[34] B. Sibbitt, D. Mcclenahan, R. Djebbar, J. Thornton, B. Wong, J. Carriere, J. Kokko, The Performance of a High Solar Fraction Seasonal Storage District Heating System – Five Years of Operation, vol. 30, 2012, pp. 856–865, https://doi.org/10.1016/j.egypro.2012.11.097.
[35] L.T. Terziotti, M.L. Sweet, J.T.M. Jr, W. Grace, Modeling seasonal solar thermal energy storage in a large urban residential building using TRNSYS 16, Energy Build. 45 (2012) 28–31, https://doi.org/10.1016/j.enbuild.2011.10.023.
[36] V. Tulus, D. Boer, L.F. Cabeza, L. Jiménez, G. Guillén-gosálbez, Enhanced thermal energy supply via central solar heating plants with seasonal storage : a multi-objective optimization approach, Appl. Energy 181 (2016) 549–561, https://doi.org/10.1016/j.apenergy.2016.08.037.
[37] D. Panno, A. Buscemi, M. Beccali, C. Chiaruzzi, G. Cipriani, G. Ciulla, M. Bonomolo, A solar assisted seasonal borehole thermal energy system for a non-residential building in the Mediterranean area, Sol. Energy (June) (2018) 0–1, https://doi.org/10.1016/j.solener.2018.06.014.
[38] R. Renaldi, D. Friedrich, Techno-economic analysis of a solar district heating system with seasonal thermal storage in the UK, Appl. Energy 236 (December 2018) (2019) 388–400, https://doi.org/10.1016/j.apenergy.2018.11.030.
[39] C.N. Antoniadis, G. Martinopoulos, Optimization of a building integrated solar thermal system with seasonal storage using TRNSYS, Renew. Energy 137 (2019) 56–66, https://doi.org/10.1016/j.renene.2018.03.074.
[40] A. Rosato, A. Ciervo, G. Ciampi, M. Scorpio, S. Sibilio, Impact of seasonal thermal energy storage design on the dynamic performance of a solar heating system serving a small-scale Italian district composed of residential and school buildings, J. Energy Storage 25 (March) (2019) 100889, https://doi.org/10.1016/j.est.2019.100889.
[41] C. Naranjo-Mendoza, M.A. Oyinlola, A.J. Wright, R.M. Greenough, Experimental study of a domestic solar-assisted ground source heat pump with seasonal underground thermal energy storage through shallow boreholes, Appl. Therm. Eng. 162 (August) (2019) 114218, https://doi.org/10.1016/j.applthermaleng.2019.114218.
[42] U. Mlakar, R. Stropnik, R. Koželj, S. Medved, U. Stritih, Experimental and numerical analysis of seasonal solar-energy storage in buildings, Int. J. Energy Res. (January) (2019) 6409–6418, https://doi.org/10.1002/er.4449.
[43] V. Rostampour, M. Jaxa-Rozen, M. Bloemendal, J. Kwakkel, T. Keviczky, Aquifer Thermal Energy Storage (ATES) smart grids: large-scale seasonal energy storage as a distributed energy management solution, Appl. Energy 242 (March) (2019) 624–639, https://doi.org/10.1016/j.apenergy.2019.03.110.
[44] A. Vallati, P. Ocłoń, C. Colucci, L. Mauri, R. de Lieto Vollaro, J. Taler, Energy analysis of a thermal system composed by a heat pump coupled with a PVT solar collector, Energy 174 (2019) 91–96, https://doi.org/10.1016/j.energy.2019.02.152.
[45] CORDIS, Effective integration of seasonal thermal energy storage systems in existing buildings, 2016. https://cordis.europa.eu/result/rcn/185046_en.html [accessed 7 October 2018].
[46] Effective integration of seasonal thermal energy storage systems in existing buildings, 2016. http://einstein.dappolonia-innovation.com/einstein-dst/main.jsf [accessed 14 September 2018].
[47] Solites - Steinbeis Research Institute for Solar and Sustainable Thermal Energy Systems, Solar DH online tool. http://www.sdh-online.solites.de/Tool/2#step-1.
[48] M. Guadalfajara, M.A. Lozano, L.M. Serra, Simple calculation tool for central solar heating plants with seasonal storage, Sol. Energy 120 (2015) 72–86, https://doi.org/10.1016/j.solener.2015.06.011.
[49] B. Rezaie, B.V. Reddy, M.A. Rosen, Assessment of the thermal energy storage in Friedrichshafen district energy systems, Energy Procedia 116 (2017) 91–105, https://doi.org/10.1016/j.egypro.2017.05.058.
[50] P. Sorknæs, Simulation method for a pit seasonal thermal energy storage system with a heat pump in a district heating system, Energy 152 (2018) 533–538, https://doi.org/10.1016/j.energy.2018.03.152.
[51] D. Mangold, T. Schmidt, Saisonale Wärmespeicher: Neue Pilotanlagen im Programm Solarthermie2000plus und Forschungsperspektiven. Statusseminar Thermische Energiespeicher, 2006, 2.-3. Nov. 2006, Freiburg, http://www.solites.de/download/literatur/06-StatusseminarTES.pdf.
[52] N. Fisch, R. Kübler, Solar assisted district heating -status of the projects in Germany, Int. J. Sol. Energy 18 (4) (1997) 259–270, https://doi.org/10.1080/01425919708914322.
[53] T. Schmidt, J. Nussbicker, S. Raab, Monitoring results from German central solar heating plants with seasonal storage, in: ISES 2005 Solar World Congress 2005, 2005. http://www.swt-stuttgart.de/SWT-Forschung/Veroeffentlichungen/Puplic/05-03.pdf.
[54] H. Müller-Steinhagen, D. Bauer, W. Heidemann, R. Marx, J. Nußbicker-Lux, F. Ochs, V. Panthalookaran, S. Raab, Solar unterstützte Nahwärme und Langzeit-Wärmespeicher, 2008. http://www.solites.de/download/literatur/ABSUN%20V%20FKZ%200329607F.pdf [accessed 21 January 2019].
[55] F. Ochs, W. Heidemann, H. Müller-Steinhagen, Modeling large-scale seasonal thermal energy stores, n.d. https://talon.stockton.edu/eyos/energy_studies/content/docs/effstock09/Session_8_2%20Models_and_Design%20tools/67.pdf.
[56] D. Mangold, T. Schmidt, The next generations of seasonal thermal energy storage in Germany, 2000. http://www.solites.de/download/literatur/07-Mangold_ESTEC%202007.pdf.
[57] Danish Energy Agency, Long term storage and solar district heating, 2017. https://ens.dk/sites/ens.dk/files/Forskning_og_udvikling/sol_til_fjernvarme_brochure_endelig.pdf.
[58] Long term storage and solar district heating: a presentation of the Danish pit and borehole thermal energy storages. Plan Energi. (n.d.). https://ens.dk/sites/ens.dk/files/Forskning_og_udvikling/sol_til_fjernvarme_brochure_endelig.pdf.
[59] Solar marstal, Summary technical description of the SUNSTORE 4 plant in Marstal, 2018. https://www.solarmarstal.dk/media/6600/summary-technical-description-marstal.pdf.
[60] T. Schmidt, P.A. Sorensen, Monitoring results from large scale heat storages for district heating in Denmark, in: 14th International Conference on Energy Storage, Adana, Turkey, 25-28 April 2018, 2018. http://planenergi.dk/wp-content/uploads/2018/05/Schmidt-and-Soerensen_Monitoring-Results-from-Large-Scale-Heat-storages.pdf.
[61] T. Schmidt, Monitoring results Marstal 2015, 2018. http://www.varmelagre.dk/files/files/Marstal/Marstal_2014-2015.pdf.
[62] P.A. Sørensen, T. Schmidt, Design and construction of large scale heat storages for district heating in Denmark, in: 14th International Conference on Energy Storage 25-28 April 2018, Adana, TURKEY, 2018. http://planenergi.dk/wp-content/uploads/2018/05/Soerensen-and-Schmidt_Design-and-Construction-of-Large-Scale-Heat-Storages-12.03.2018-004.pdf.
[63] P.A. Soerensen, M. Vang Jensen, Smart district heating using the SUNSTORE concept, Strojarstvo 54 (6) (2013) 455–461. From, N,. Paper, https://hrcak.srce.hr/file/144638.
[64] PlanEnergi SUNSTORE 4, Deliverable D.2.2, Version 3: Design of the Pit Heat Storage of the Demonstration Plant at Marstal Fjernvarme, 2013.
[65] A.J. Dannemand, L. Bødker, M.V. Jensen, Large thermal energy storage at Marstal district heating, in: Proceedings of the 18th International Conference on Soil Mechanics and Geotechnical Engineering, Paris 2013, 2013. http://www.cfms-sols.org/sites/all/lic/pages/download_pdf.php?file=3351-3354.pdf.
[66] D. Mangold, O. Miedaner, E.P. Tziggili, T. Schmidt, M. Unterberger, B. Zeh, Technisch-Wirtschaftliche Analyse Und Weiterentwicklung Der Solaren Langzeit-Wärmespeicherung. Steinbeis Forschungsinstitut für solare und zukunftsfähige thermische Energiesysteme, 2011. Stuttgart, http://www.solites.de/download/literatur/Solites_Technisch-wirtschaftliche%20Analyse%20und%20Weiterentwicklung%20der%20solaren%20Langzeit-W%C3%A4rmespeicherung_Forschungsbericht_FKZ%200329607N_2012.pdf.
[67] SIA Standard 381/3: Heating Degree-Days in Switzerland, Swiss Association of Engineers and Architects, Zurich, Switzerland, 1982 (in German).
[68] Energy PLAN, Department of development and planning, Aalborg University (n.d.), https://www.energyplan.eu/. (Accessed 14 September 2018).
[69] H.O. Njoku, O.V. Ekechukwu, S.O. Onyegegbu, Analysis of stratified thermal

Please cite this article as: K. Narula et al., Simulation method for assessing hourly energy flows in district heating system with seasonal thermal energy storage, Renewable Energy, https://doi.org/10.1016/j.renene.2019.11.121

storage systems: an overview -heat & mass transfer, 50, 2014, pp. 1017–1030, https://doi.org/10.1007/s00231-014-1302-8, 7.
[70] Y.M. Han, R.Z. Wang, Y.J. Dai, Thermal Stratification within the Water Tank, vol. 13, 2009, pp. 1014–1026, https://doi.org/10.1016/j.rser.2008.03.001.
[71] J. Fan, J. Huang, A. Chatzidiakos, S. Furbo, Experimental and theoretic investigations of thermal behaviour of a seasonal water pit heat storage, in: Paper Presented at Solar World Congress 2017, Abu Dhabi, United Arab Emirates, 2017. http://orbit.dtu.dk/files/141970828/Untitled_2.pdf.
[72] J.-C. Hadorn, Guide du stockage saisonnier de chaleur, Documentation D028: SIA, Société suisse des ingénieurs et architectes, Zurich, 1988.

Please cite this article as: K. Narula et al., Simulation method for assessing hourly energy flows in district heating system with seasonal thermal energy storage, Renewable Energy, https://doi.org/10.1016/j.renene.2019.11.121